Measurements interpretations of tilt–strain gauges in seismically active areas

Article *in* Earth-Science Reviews · September 1999

DOI: 10.1016/S0012-8252(99)00028-8

2 authors, including:

Carla Braitenberg
University of Trieste
168 PUBLICATIONS **2,970** CITATIONS

ELSEVIER

Earth-Science Reviews 47 (1999) 151–187

EARTH-SCIENCE REVIEWS

www.elsevier.com/locate/earscirev

Measurements and interpretations of tilt–strain gauges in seismically active areas

Maria Zadro *, Carla Braitenberg

Department of Earth Sciences, University of Trieste, Via Weiss 1, 34100 Trieste, Italy

Received 15 May 1998; accepted 13 April 1999

Abstract

An overview of different aspects of deformation measurements is given. An introduction to the general theory of point-crustal deformations with an application to the stress–strain relations at the earth surface is made. The instrumentation used in crustal deformation measurements is briefly explained, emphasizing different constructions of tilt and strainmeters. The problems connected with the housing of the instruments, i.e., the cavity and topography effects, and with the ambient noise factors, as the hydrological and pressure effects, are discussed. The last part of the paper is concerned with the relation between deformation measurements and seismic events, both from a theoretical and observational standpoint. A number of examples are shown that report on pre-, co-, and post-seismic and the secular term deformation in different areas of the world.

Keywords: deformation; strainmeters; tiltmeters; precursors; co-seismic processes

1. Introduction

In the last few decades, strain and tilt measurements have been made throughout the world. A strong impulse to the installation of a great number of stations occurred after the year 1957, designated as the 'International Geophysical Year' by IUGG. In the frame of the 'International Geophysical Year' the IAG (International Association of Geodesy) decided to improve the earth tides measurements and the International Centre for Earth Tides was founded in Bruxelles.

The target for a tilt–strain station can be very diversified, according to the specific location chosen, which can be either a seismically active (including volcanism and high seismic potential) or inactive (no occurrence of earthquakes) area. To cover all the different aspects of strain/tilt measurements, the contents of an entire volume may be easily filled: reportedly (Varga, 1984) in the year 1984, 150 crustal strain stations were

* Corresponding author. Tel.: +39-040-6762258; Fax: +39-040-575519; E-mail: zadro@univ.trieste.it or carla@geosun3.univ.trieste.it

0012-8252/99/$ - see front matter
PII: S0012-8252(99)00028-8

operative throughout the world. Our task to review strain/tilt measurements in a journal paper implies narrowing the field of interest.

We have chosen to discuss measurements which have been carried out in seismically active areas, with the aim to provide information on the results regarding the relation between the different stages of the earthquake cycle and the crustal deformation measurements. This includes the deformations during the pre-, co-, and post-seismic phases. At first, a general introduction to stress–strain relations is given, and a discussion of the quantities measured by tiltmeters and strainmeters is made. A short overview of the different instruments used in the observation stations follows, including the problems connected to the housing of the instruments in cavities, mines or boreholes.

As a rule, deformation measurements are affected by natural noise induced by atmospheric agents at frequencies near the tectonic signals. It seems that one of the major problems in the identification of pre- or post-seismic signals is that these, if fortuitously present, have similar signatures as the hydrologically induced signals. Consequently, in many cases, it is difficult or even impossible to prove the statistical reliability of a

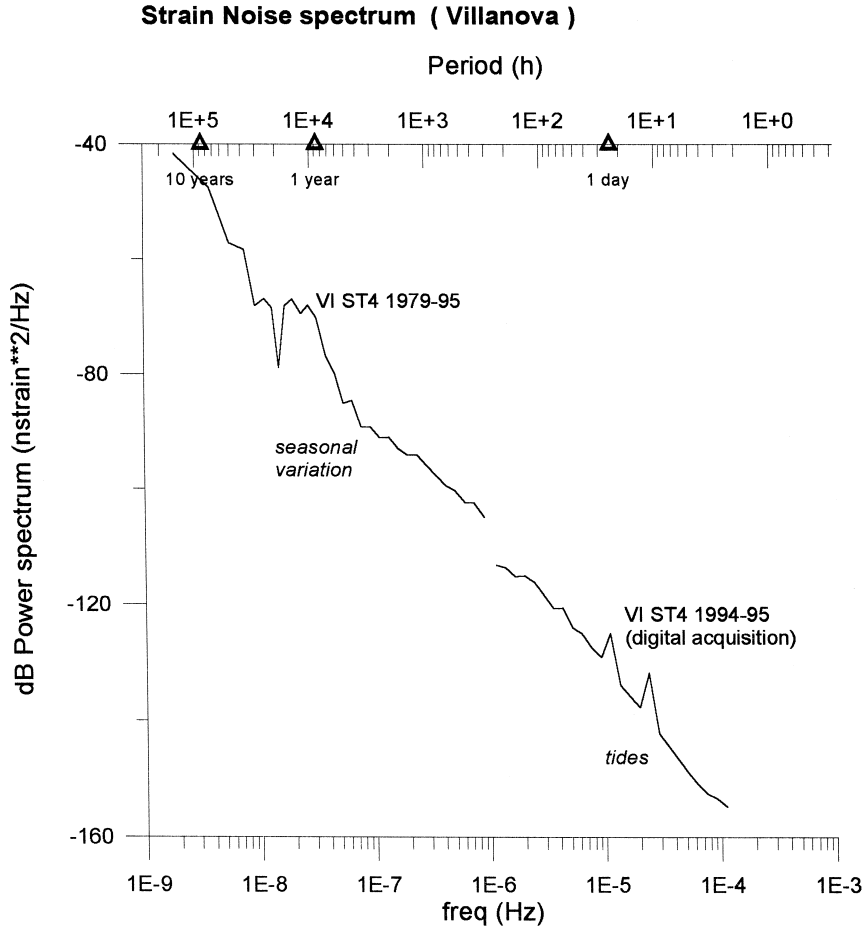

Fig. 1. Noise spectrum for horizontal wire strainmeter measurements. The spectrum is calculated on for the frequency interval 10^{-9}–10^{-4} and on hourly sampled data for the interval 10^{-9}–10^{-4}. The noise level is lower for the more recent (1994–1995) years with respect to the entire dataset (1977–1995), due to the change from optical to digital acquisition system.

deformation signal observed near the occurrence time of a seismic event. We discuss the different techniques used for identifying and modelling the induced signals. Unfortunately, the most disturbing factor, the hydrologically induced deformation, cannot be reliably modelled due to its highly nonlinear character. Finally, we reach the main topic, the tectonic deformation, which we discuss first from a theoretical standpoint in order to evaluate the signals that may be expected. Then we pass on to the observations, divided into short-term to mid-term and secular observations.

Inevitably, any narrowing of the field which is going to be treated results in excluding a number of well and long-term operating stations from the discussion, and we apologize for this fact. An important application of strain–tilt measurements, not included in this review, is the measurement of earth tides. A number of stations has been deployed specifically for this topic, in seismically active and inactive areas. These studies are easily accessible in both exhaustive literature (e.g., Melchior, 1983), and specific journals (e.g., *Bulletin d'Information de Marées Terrestres*). Another important application of strain measurements is connected to mining activities and to the monitoring of the stability of mines. A wide use of deformation measurements is made in volcanic

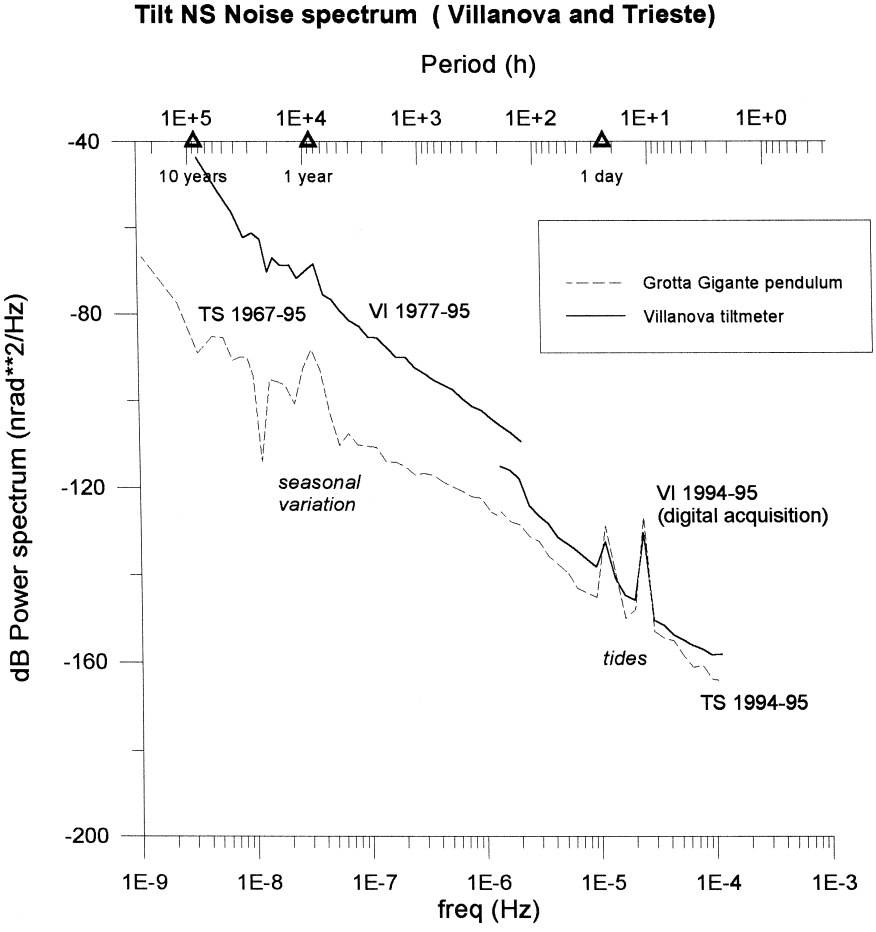

Fig. 2. Noise spectrum for Zöllner-type tilt measurements. The spectrum is calculated on daily sampled data for the frequency interval 10^{-9}–10^{-4} and on hourly sampled data for the interval 10^{-9}–10^{-4}. As for the strainmeter (Fig. 1) also for the VI-tilt the noise level is lower for the year 1994–1995, due to the improved acquisition system.

studies, which opens an entire chapter for itself, and which could only marginally be included in the present review.

In the past, some reviews on deformation measurements in connection to earthquakes have been made. In particular, studies have focused on the collection and critical evaluation of reports on earthquake precursors. Papers dated prior to 1976 can be found in Rikitake (1976), more recent papers in the AGU volume on Earthquake Prediction as, e.g., in Bilham (1981) and Mogi (1981). A recent review of measurements of geodynamical interest is by Zürn (1994).

Before entering a detailed discussion, we present the typical spectra of continuous extensometric and tilt records. Fig. 1 shows the noise power spectrum of an invar wire strainmeter installed in a natural cavity in the Southern Alps. The spectrum was calculated from 17 years of daily sampled data for the low frequencies (10^{-9} to 10^{-6} Hz) and on 2 years of hourly sampled data for the higher frequencies (10^{-6} to 10^{-4} Hz). The noise reduction due to the improvement of the data acquisition system from optical to digital recording is seen in the jump when passing from the low-frequency part (optical and digital recording) to the higher-frequency part (only digital recording). The most significant deviations from the linear dependence of spectral density on frequency in the graph drawn in logarithmic scale are due to tides (diurnal and semidiurnal variation) and due to the seasonal cycle. The tilt power spectrum is shown in Fig. 2. Two Zöllner-type tiltmeters of very different dimensions, both installed in natural cavities, are compared: the TS instrument uses a baseline of 100 m and the VI instrument of 60 cm. The main features found for the extensometer records are observed also in the tilt spectra. The longer baseline instrument (TS) has a much lower noise level, particularly at low frequency when compared to the short base instrument.

2. Point-crustal deformations

2.1. Deformation matrices

The interpretation of strain and tilt-meter data in terms of strain and rotation rate is presented in the present paragraph assuming homogeneous deformation. The influence of surrounding inhomogeneities and the depth of the measurement point will be treated later on.

Consider the case of infinitesimal deformations in 3D, with $\mathbf{J}$ the 3×3 Jacobian matrix (or displacement gradient matrix) associated with the displacement field $\vec{u}$ in the Cartesian coordinate system $\vec{x}$. Elements of $\mathbf{J}$ are $\partial u_x/\partial x$, $\partial u_x/\partial y$, etc., according to usual notations.

The matrix can be written as the sum of a symmetric matrix $\mathbf{E}$ and a skew-symmetric matrix $\boldsymbol{\Omega}$ (see e.g., Malvern, 1969, p. 120–135) $\mathbf{J} = E + O$, where $\mathbf{E} = 1/2(\mathbf{J} + \mathbf{J}^{\mathrm{T}})$ and $\boldsymbol{\Omega} = 1/2(\mathbf{J} + \mathbf{J}^{\mathrm{T}})$.

The matrix elements of $\mathbf{E}$ and $\boldsymbol{\Omega}$ are:

$$\mathbf{E} = \begin{bmatrix} \varepsilon_{xx} & \varepsilon_{xy} & \varepsilon_{xz} \\ \varepsilon_{yx} & \varepsilon_{yy} & \varepsilon_{yz} \\ \varepsilon_{zx} & \varepsilon_{zy} & \varepsilon_{zz} \end{bmatrix} = 1/2 \begin{bmatrix} 2(\partial u_x/\partial x) & (\partial u_x/\partial y + \partial u_y/\partial x) & (\partial u_x/\partial z + \partial u_z/\partial x) \\ (\partial u_x/\partial y + \partial u_y/\partial x) & 2(\partial u_y/\partial y) & (\partial u_z/\partial y + \partial u_z/\partial y) \\ (\partial u_x/\partial z + \partial u_z/\partial x) & (\partial u_z/\partial y + \partial u_z/\partial y) & 2(\partial u_z/\partial z) \end{bmatrix} \tag{1}$$

$$\mathbf{\Omega} = \begin{bmatrix} \omega_{xx} & \omega_{xy} & \omega_{xz} \\ \omega_{yx} & \omega_{yy} & \omega_{yz} \\ \omega_{zx} & \omega_{zy} & \omega_{zz} \end{bmatrix} = 1/2 \begin{bmatrix} 0 & (\partial u_x/\partial y - \partial u_y/\partial x) & (\partial u_x/\partial z - \partial u_z/\partial x) \\ (\partial u_y/\partial x - \partial u_x/\partial y) & 0 & (\partial u_y/\partial z - \partial u_z/\partial y) \\ (\partial u_z/\partial x - \partial u_x/\partial z) & (\partial u_z/\partial y - \partial u_y/\partial z) & 0 \end{bmatrix} \tag{2}$$

The symmetric matrix **E** represents a second order symmetric tensor (the irrotational strain tensor) and $\boldsymbol{\Omega}$ a second order skew-symmetric rotation matrix. The diagonal elements of **E** are the longitudinal strains along the cartesian coordinate directions, the trace of **E** gives the first strain invariant Δ (invariant with respect to whatever rotation of the reference system) which corresponds to the dilatation of the deformation, whereas the off-diagonal elements are the shear components of the strain itself. The rotational vector is represented by the ω_{xy}, ω_{xz}, ω_{yz} elements.

The principal strains of the deformation are defined as the eigenvalues of the **E**-matrix, and the principal directions of strains as the orientations of the eigenvectors. The principal strains are denoted by ε_1, ε_2, ε_3 with the convention $\varepsilon_1 \geq \varepsilon_2 \geq \varepsilon_3$. The *xy*, *yz*, *zx* coordinate planes represent the 'principal planes' of deformation.

Unfortunately, a discrepancy exists in literature in the definition of the shear components (off diagonal elements of **E**), for which sometimes the $1/2$ factor in Eq. (1) is omitted.

From the above defined 3 by 3 **J**, **E** and $\boldsymbol{\Omega}$ matrices, it follows that in general there are nine unknowns so that nine independent measurements should be necessary in order to have a complete description of the deformation. The theoretically easiest and the most natural way to get a complete description of the **E** matrix should be the one given by a set of six strainmeters suitably oriented (no parallel orientations, not more than three coplanar), or by a set of five strainmeters and one dilatometer, the last giving the first strain invariant. Moreover, by adding two tiltmeters, one can also obtain the elements ω_{xz}, ω_{yz} of $\boldsymbol{\Omega}$, whereas the rotation about the vertical axis cannot be detected by present instruments. Regarding tectonic problems, in which the rotational component regards slow movements spread over large time intervals, the rotation can be obtained step by step from the rotation of the triade of principal axes ε_1, ε_2, ε_3.

Due to technical, logistic and economical reasons, a complete set of instruments (six strainmeters or five strainmeters and one dilatometer, 2 tiltmeters) has never been installed anywhere up to now. But it has to be noted that theoretical considerations and assumptions on the stress–strain field, acceptable for surface or subsurface measurements, allow us to reduce the number of the unknown elements of the **J** or **E** and $\boldsymbol{\Omega}$ matrices. They are treated in the following.

2.2. Stress–strain relationships at the earth surface

Let us consider the stress matrix and the corresponding stress–strain relationships in the *x y z* coordinate system, employing the usual notations:

$$\boldsymbol{\Sigma} = \begin{vmatrix} \sigma_x & \tau_{xy} & \tau_{xz} \\ \tau_{yx} & \sigma_y & \tau_{yz} \\ \tau_{zx} & \tau_{zy} & \sigma_z \end{vmatrix}. \tag{3}$$

The matrix $\boldsymbol{\Sigma}$ is symmetric, with $\tau_{xy} = \tau_{yx}$, $\tau_{xz} = \tau_{zx}$, $\tau_{yz} = \tau_{zy}$ as the shear stress components and σ_x, σ_y, σ_z as the normal stresses.

Due to boundary conditions, at the free surface $\sigma_z = 0$, $\tau_{xz} = 0$, $\tau_{yz} = 0$. σ_x, σ_y, τ_{xy} depend upon tectonic and local stresses.

The stress–strain relationships for an isotropic elastic model (Hook's law) result as (e.g., Jaeger, 1983, p. 56):

$$\begin{aligned} \sigma_x &= \lambda\Delta + 2\mu\varepsilon_{xx} \\ \sigma_y &= \lambda\Delta + 2\mu\varepsilon_{yy} \\ \sigma_z &= \lambda\Delta + 2\mu\varepsilon_{zz} \end{aligned} \tag{4}$$

$$\tau_{xy} = 2\mu\varepsilon_{xy}, \tau_{xz} = 2\mu\varepsilon_{xz}, \tau_{yz} = 2\mu\varepsilon_{yz} \tag{5}$$

with Δ the dilatation or first invariant ($\Delta = \varepsilon_{xx} + \varepsilon_{yy} + \varepsilon_{zz}$), and μ the Lamé parameters. The factor 2 in Eq. (5) is sometimes omitted in literature (as in Jaeger) as a consequence of the already noted difference in the definition of the shearing strain.

In the homogeneous and isotropic elastic linear case, it is assumed that the principal axes of strain are coaxial with the principal axes of stress. Definitions analogous to the strain field are valid for principal stresses, principal planes and principal directions. Due to boundary conditions, taking into account the earth's gravity field, at the free surface one principal axis of the stress (and therefore of the strain) has to be vertical. Moreover, the normal stress has to be equal to zero as well as the shearing stresses acting along whatever vertical plane.

For the above reasons, and according to the notation generally used in tilt–strain measurements, we will adopt the Local Geodetic reference in the sequel, defined with the z axis upwards oriented, and x and y the E–W and N–S horizontal axes (E and N positive), respectively.

2.3. Information on the deformation state from tilt–strain measurements

One tiltmeter allows to record only one off-diagonal element of the Jacobian displacement gradient matrix, and a couple of tiltmeters oriented, as usual, according to the E–W and N–S cardinal directions give two elements of the matrix, $\partial u_z/\partial x$ and $\partial u_z/\partial y$, respectively (e.g., Rodgers, 1968). Of course in one station two tiltmeters are sufficient in order to obtain the maximum information available from this kind of instruments. This is so because the tilt is a vector in the horizontal plane, and two orthogonal components allow us to compute the tilt along whatever azimuth. Although the interpretation of tilt data is very natural in terms of the Jacobian matrix elements, it is not so when considering them in terms of shearing and rotation. Neglecting Earth-tide effects (which are beyond the present discussion and have to be filtered out from the records) the depth of the station has to be taken into account, and, moreover, a consideration of particular stress–strain regional situations can be of great help in the interpretation of the time evolution of the deformational state (Ebblin and Zadro, 1979; Ebblin, 1986; Zadro, 1992). Let us employ such an approach in the sequel.

If we are at the free surface of the Earth, due to boundary conditions and considering Eq. (5), both ε_{xz} and ε_{yz} have to vanish, so that with the definitions of Eqs. (1) and (2):

$$\frac{\partial u_z}{\partial x} = \frac{-\partial u_x}{\partial z}; \quad \frac{\partial u_z}{\partial y} = \frac{-\partial u_y}{\partial z} \tag{6}$$

and

$$\omega_{xz} = \frac{\partial u_z}{\partial x}; \quad \omega_{yz} = \frac{\partial u_z}{\partial y} \tag{7}$$

Reminding that tiltmeters measure $\partial u_z/\partial x$ and $\partial u_z/\partial y$, it follows from Eq. (7) that these instruments at the Earth free surface measure pure rotation only.

A different situation occurs when we consider a station at even a shallow depth (z) below the earth's surface. The above boundary conditions are no more valid, since $\sigma_z = \rho g z$ (ρ crustal density, g gravity) and for a Poisson condition ($\lambda = \mu$) the horizontal principal stresses should be roughly $1/3$ of the vertical principal stress, although there is evidence that even at depths involved in mining, the stresses are sometimes already near to hydrostatic values (Jaeger, 1983, pp. 120–121). Hast (1973) has performed absolute stress borehole measurements in several areas up to the depth of 2500 m and has shown that the predominant stresses in the upper part of the earth's crust are in general horizontal, and that at the ground level the sum $\sigma_x + \sigma_y$ is about 20 MPa. At depth this value increases linearly and is stabilized by the weight of the overburden.

In the particular case that the strainfield can be assumed as irrotational, the $\mathbf{\Omega}$-matrix is equal to zero. In this hypothesis ω_{xz} and ω_{yz} will disappear so that:

$$\frac{\partial u_z}{\partial x} = \frac{\partial u_x}{\partial z}; \quad \frac{\partial u_z}{\partial y} = \frac{\partial u_y}{\partial z} \tag{8}$$

$$\varepsilon_{xz} = \frac{\partial u_z}{\partial x}; \quad \varepsilon_{yz} = \frac{\partial u_z}{\partial y} \tag{9}$$

In underground cavities, a station equipped with a set of six strainmeters forming a tetrahedron, is sufficient to give all the components of the irrotational strain tensor. However, several difficulties of both practical and technical nature discourage the employment of such kind of fully equipped stations.

The most common disposition is of one, two or three strainmeters located in the horizontal plane. The longitudinal strain can thus be measured along one, two or three horizontal directions: in the last case the horizontal components of the irrotational tensor can be found, provided that the three directions be different. The areal horizontal dilatation then is obtained from the sum of the two principal horizontal strains. If in the case of three horizontal strainmeters a couple of tiltmeters are added, then the determination of the strain tensor is improved by two components, so that such an equipment allows the determination of all but one (ε_{zz}) of the six strain tensor components.

In practice, it may be possible to apply particular assumptions about the strain state, as the assumption of equivolume, plane strain, axial strain or about the tectonic stress field, as plane stress, axial stress and the stress–strain relationship (Hook's law). This implies a linear relationship between the principal strains (Eq. (4)), and a reduction of the number of unknowns. As already noted, the availability of one dilatometer can as well reduce the number of unknowns by one.

In the case of surface measurements, for which $\sigma_z = 0$, $\tau_{xz} = 0$, $\tau_{yz} = 0$, with the above instrumentation (three horizontal strainmeters and a couple of tiltmeters), again all the $\mathbf{E}$ and $\mathbf{\Omega}$ matrix elements but one (ε_{zz}) can be found.

3. The instruments

Deformation of the crust can be measured in many ways, including the geodetic surface campaigns and the surface and subsurface strain and tilt measurements. In geodetic measurements, the time variation of relative distances of benchmark stations of a network are given by distance measurements which have also extended over several decades. The distance measurements over the network can be used to calculate the mean strain rate tensor (e.g., Prescott et al., 1979), which represents the surface deformation averaged over a network. Classical measurements are made on levelling, trilateration and triangulation networks, which today are mostly being replaced by GPS (Global Positioning System), VLBI (Very Long Base Interferometry) and SLR (Satellite Laser Ranging) measurements (e.g., Pearson et al., 1995; Savage et al., 1995). The integration of older geodetic measurements with the recent GPS measurements allows to trace the evolution of the strain rate tensor in some areas over the past several decades (Bawden et al., 1997) up to the present. In the present paper though, we emphasise the techniques and applications of subsurface measurements and give a brief overview of the instrumentation used in underground strain and tilt measurements. The deformations to be measured are of the order of 10^{-8} for earth tides (tens of milliseconds for tiltmeters) and are variable for tectonic short, mid and secular terms. For technical instrumental details we refer to the benchmark paper on tilt and strainmeters by Agnew (1986).

3.1. Tiltmeters

The tiltmeter is designed to measure the tilt of a horizontal base. Instrumental designs differ greatly, depending on the use and resolution necessary for the particular application. Volcanic measurements require robust installations, and not very high sensitivity, whereas the measurements of tidal tilts and long-period tectonic movements, require stable and highly sensitive measurements. Most common are point measurements, by short baseline instruments, in which the inclination of the plane is measured by a vertical or horizontal pendulum, or by bubble tiltmeters.

For vertical pendulums, the boom holding the mass is suspended vertically, and the relative variation of boom inclination with respect to a reference axis fixed to the ground which was mounted along the surface

normal, is measured. For static deformations, that is, slow movements with respect to the eigenfrequencies of the pendulum system, the measured angle gives directly the tilt angle. Small compact instruments are set into boreholes (Flach, 1976; Levine et al., 1989), or longer instruments are suspended in cavities (Schmitz-Hübsch, 1986; Vieira et al., 1991).

Horizontal pendulums suspend the boom horizontally, according to the principle of the Zöllner-type suspension (Fig. 3). A ground tilt leads to a greatly amplified rotation angle of the boom in the subhorizontal plane. For static deformations, the amplification is $1/\sin(i)$, i being the inclination of the (ideal) rotation axis of the boom with respect to the vertical. The variation of the amplification with tilt, and thus with time, makes periodic calibration necessary. The inclination angle (i) may be obtained by measuring the free (T) of the pendulum, which is equal to:

$$T = 2\pi\sqrt{\frac{l}{g\sin(i)}}\,, \tag{10}$$

with l being the reduced pendulum length, g the gravity at the observation site (e.g., Melchior, 1983). The reduced pendulum length (l) is a non-time varying characteristic of the pendulum and can be measured in the laboratory. An alternative calibration method is to apply a known tilt to the instrument, and measure the recorded tilt. As for sensitive instruments, the tilts involved are very small, the precisely calculated deformation to a known stress is used as the input signal (crapoudine) (Verbaandert, 1962; Melchior, 1983). The horizontal

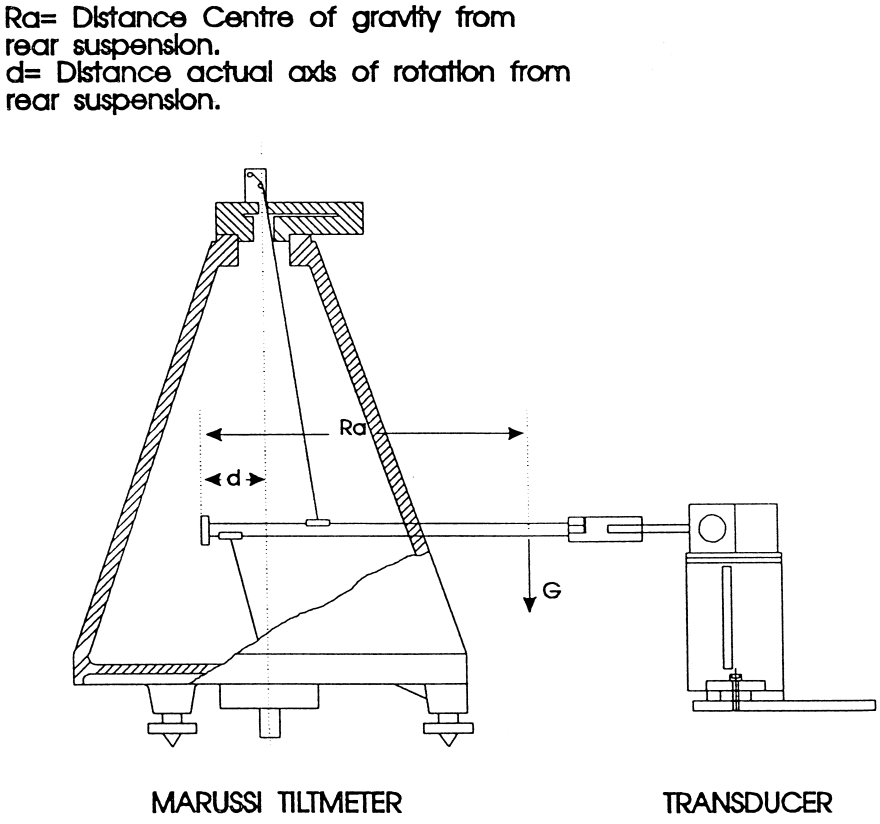

Fig. 3. Schematic diagram of a horizontal pendulum of Zöllner-type suspension.

component seismometers operate on the same principle as the horizontal pendulums, to record the horizontal component of ground displacement, velocity or acceleration.

The problem of the variation of the amplification factor with tilt is removed by applying a feedback system, which keeps the boom in a defined position, leading to a constant sensitivity (van Ruymbeke and d'Oreye, 1991).

The sizes and masses of the tiltmeters vary from miniature instruments (7 cm across) (Agnew, 1986; Delorme and Blum, 1991), to medium-sized instruments like the widely used Verbaandert Melchior (VM) Tiltmeters (Ostrovsky, 1961; Verbaandert and Melchior, 1961), to larger constructions as the Marussi Pendulums (Zadro, 1978). Of exceptionally large dimensions are the horizontal pendulums of the Trieste Grotta Gigante cave, operative since 1958. Both upper and lower suspensions are attached to the rock of the cave, at 95 m height difference (Marussi, 1960). The mass of the pendulums is 14 kg. Due to their exceptional characteristics, these instruments furnished the best records of the lowest order torsional-free oscillations of the earth generated by the great Chile 1960 earthquake (Bolt and Marussi, 1962).

The bubble tiltmeters (e.g., Kinemetrics; Hughes: Groten (1980), p. 679) are compact instruments which do not necessitate particularly sheltered housing. The motion of a bubble trapped by a slightly curved surface is sensed. The bubble movement is greater for small curvatures of the curved surface. Borehole installations are discussed in (Wyatt et al., 1988).

Compared to the short baseline tiltmeters, the water-tube tiltmeters can be built to measure tilt across a long baseline. A fluid surface is used as a reference for measuring the differential fluid level at two points. A natural tiltmeter of this sort is a lake, the differential water level in two points at opposite shores of which, gives the tilt along the line connecting the two points (Mueller et al., 1989). In tube-tiltmeters, the fluid levels at both ends of the tube are measured (Michelson, 1914; Hagiwara, 1947; Eaton, 1959). Alternatively, the two fluid level measurements are substituted with only one measurement of the pressure difference to both sides of the centre of the instrument (Horsfall and King, 1977).

Comparison of tidal tilts measured by short base line tiltmeters and a 170-m-long baseline tube tiltmeter in the Black Forest Observatory revealed that the latter agreed much better with the tidal tilts predicted from an elastic earth model (Zürn et al., 1986).

3.2. Strainmeters

Strainmeters are built to measure the time variation of either linear strain, areal strain, shear strain, or volumetric strain. Largely used for geophysical purposes are extensometers, which measure the variation of distance between two fixed points in cavities, mines, or trenches (or, occasionally, on the surface). Extensometers are mounted horizontally or vertically. The resolution required for the study of tectonic and tidal strains is 10^{-9}. Early extensometers had been built for measuring seismic strains (Benioff, 1935), and consisted of a solid rod (20 m long iron pipe) and a velocity transducer. Later interest broadened to slower signals, and tubes or rods were made of quartz or invar, so as to be less temperature sensitive, and a displacement transducer replaced the velocity transducer. The quartz tube of Benioff probably produced the first observations of free oscillation, excited by the Kamchatka Earthquake of 1952 (Bullen and Bolt, 1985, p. 352). Doubts about the observations aroused later in 1960, when the earth's free oscillations generated by the great Chile earthquake were unambigously detected. The original data have been re-examined and discussed in (Kanamori, 1976). The rigid extensometers were widely used for long-term strain observation as in Japan (Takemoto, 1979; Kasahara et al., 1983) and in Eastern Europe (Varga and Varga, 1995).

In alternative to the difficult to transport rigid rod, a flexible wire which is usually made of Invar, quartz or carbon fibre is stretched between the two points to be measured. One important and well documented instrument is the Cambridge Invar wire strainmeter (King and Bilham, 1976).

The class of laser strainmeters date back to the 1960s, and consist of a long path Fabry–Perot or an unequal-arm Michelson interferometer. The relative variations of length are detected with a sensitivity of 10^{-12}

on baselines which range from $10^2 - 10^3$ m. The number of laser strainmeters is far smaller than the number of wire or rod strainmeters, due to the more complex construction. For further details we refer to Berger and Lovberg (1970), Levine and Hall (1972), Goulty et al. (1974), Takemoto (1979) and Dubrov and Alyoshin (1992).

Another class of strainmeters belongs to the borehole installations, which comprise the volume strainmeters and the 3-component tensor strainmeters. The principle of a volume strainmeter, the most used being the Sacks–Evertson strainmeter, consists of a closed volume containing a liquid (oil), which flows through a small hole at the top of the container in response to varying compression of the volume (Sacks and Evertson, 1968). A summary of the performance of such instruments is described in (Furuya and Fukudome, 1986), who describe the experience collected in 36 stations installed throughout Japan.

Areal or volumetric crustal strain can also be obtained from the observation of the water level of suitably chosen wells. Strain sensitivity of the water level depends on the confinement of the aquifer and on the porosity of the host rock. For a discussion, see Rojstaczer (1988) and Roeloffs and Quilty (1997). The wells studied by Rojstaczer proved to be useful as strainmeters and had comparative noise levels as wire strainmeters or dilatometers for strain events in the frequency band from 0.08 to 2.5 cycles/day.

The 3-component borehole strainmeters consist of rod strainmeters of small baselength (10^{-1} m) apt to fit into a borehole. Having 3 skew horizontal strainmeters allows to determine the areal and shear strain deformation in the horizontal plane (Gladwin et al., 1987).

3.3. Holographic measurement of strain

An interesting instrumentation for measuring crustal 2D or 3D deformation is based on holographic interferometry. The holographic virtual image of an area of the cave is superposed to the current scene of the object, producing an interference fringe pattern (Takemoto, 1990). Such an instrument was installed in 1984 in a tunnel at the Amagase Crustal Observatory, Kyoto, Japan (Takemoto, 1986). Holograms of an area 1 m × 1 m of the tunnel wall painted white is used for observations. The results are consistent with strain changes observed with the laser extensometer installed at the same site. A future application could be to investigate the cavity effect and to study the local inhomogeneities of the strain field.

Some thing should be said about units: deformation by definition is a non-dimensional quantity. Tilt is either given in radians or seconds of arc, or in the smaller unit 10^{-6} rad (micro rad) or 10^{-3} sec (msec). Strain is given in 10^{-6} or 10^{-9} (micro or nano) strain or in micro or nano rad, the latter being used to describe the angle of shear.

4. Cavity and topography effects, and site selection

The presence of a cavity modifies the strain field locally. Also the presence of a rugged topography, in which the measurements are taken, leads to a measured strain field which differs from the regional field. The above are called cavity and topography effects, respectively, and have been discussed thoroughly by Harrison (1976). Generally speaking, the strainfield inside the cavity is a linear combination of the strain components at infinity. The linear coefficients are usually referred to as strain coupling coefficients. The cavity effect of an ellipsoid has been solved analytically (Harrison, 1976), and the coupling coefficients of the strain components in the cavity to the strain tensor components at infinity can be calculated. For irregularly shaped tunnels or cavities, the coupling coefficients are obtained by finite element calculations. The cavity and topography effects have been calculated for various strain-tilt stations as in Emter and Zürn (1985) and Sato and Harrison (1990). Also local inhomogeneities of the crust can modify the observed strain signal considerably, an effect for which the finite

element technique or other numerical techniques can be used as an approach to tentatively predict the observations (e.g., Meertens et al., 1989).

Given a certain deformation characterized by the principal deformations ε_1, ε_2, ε_3, the angular variation of the normal to a hypothetic plane, depends on the orientation of the normal. In fact, the angular variation is zero for a normal aligned with the orientation of one principal axis of deformation. This fact has some consequences for the tilt measurements made in cavities. The tiltmeter measures the tilting of the tangent plane to the cavity surface in the point where the tiltmeter is fixed to. It follows then that for a given deformation state, the measured angles vary, for different orientations of the tangent plane. A discussion of this problem, with some application to the Friuli tiltmeter network has been made in Ebblin (1986) and Ebblin and Zadro (1979), where the expected tilt recorded in an ellipsoidal cavity under different possible tectonic hypotheses is discussed.

As important for the strain observation the correct functioning of the instrument is, so is the selection of the site into which the instrument is installed. Apart from theoretical considerations regarding the boundary conditions on the surface, the influence of atmospheric disturbances (temperature, barometric pressure and hydrologic influences) makes the choice of a deep installation preferable. According to Gladwin and Hart (1985), the depth of borehole installations should be at least 100 m. A recently excavated cavity is not advisable, as due to strain relaxation, the records will be affected by continuous drift (Kasahara et al., 1983) over several years. Borehole installations require filling the boreholes to the surface with concrete in order to reduce long term strain changes resulting from hole relaxation effects and to avoid strains resulting from re-equilibration of the acquifer system (Johnston et al., 1994). A discussion of the calculation of the far field strains in the host rock from the observed bore-hole cylinder deformations is given by Gladwin and Hart (1985) and Hart et al. (1996).

5. Atmospheric pressure and hydrological effects.

Both atmospheric and hydrological effects appear as ‘anomalous’ or noise signals in a broad frequency range, which includes the band of earth tides and the band of middle- to short-term seismotectonic deformations. Due to the dependence on the local geological and terrain conditions, the atmospheric and hydrological effects must be carefully studied for every observation station, in order to allow identification, and in the ideal case, separation from other signals of interest (earth tides, pre- co- post-seismic deformations).

Several problems hamper this task. The first is the correlation between barometric pressure and rainfall. The second resides in the complex relation between rainfall and water table level, relation which is nonlinear and strongly dependent on the local hydrology and the rock fabric, both generally not known in sufficient detail. A third problem, more important for earth tide studies than for long-, middle- and short-term tectonic and/or seismic deformations, regards the atmospheric tide (Chapman and Lindzen, 1970), which due to different weather conditions has variable amplitude at diurnal, semidiurnal and terdiurnal frequencies. Some authors remove the atmospheric loading strains using least squares techniques (e.g., Johnston et al., 1986)

Studies comparing barometric and hydrologic effects have shown that the hydrologic effect has a much larger amplitude than the barometric effect. Edge et al. (1981) consider nine months of borehole tilt measurements in the English Lake District. The two perpendicular tiltmeters are installed in metamorphic slate at a depth of 12 m. The analysis is carried out on the non-tidal low-frequency tilt data, comparing the data with the atmospheric pressure as well as with the rainfall and water table measurements. Tilt (channel X in Figs. 4 and 5) associated with water table variation is shown to be oriented perpendicular to the strike of the cleavage planes of the slate forming the bedrock. Parallel to the cleavage planes a 90% correlation is observed between tilt signal (channel Y) and pressure (Figs. 4 and 5). The regression coefficient for these extreme cases is about 10 nrad/mbar (2 msec/mbar) for pressure and 1 μrad/m (200 ms/m) for watertable variations. This amounts to a ratio of pressure and hydrologic induced signal of about 1:10, which makes the pressure induced signal negligible with respect to the hydrologically induced signal. A similar study was conducted (Dal Moro and Zadro, 1998) on

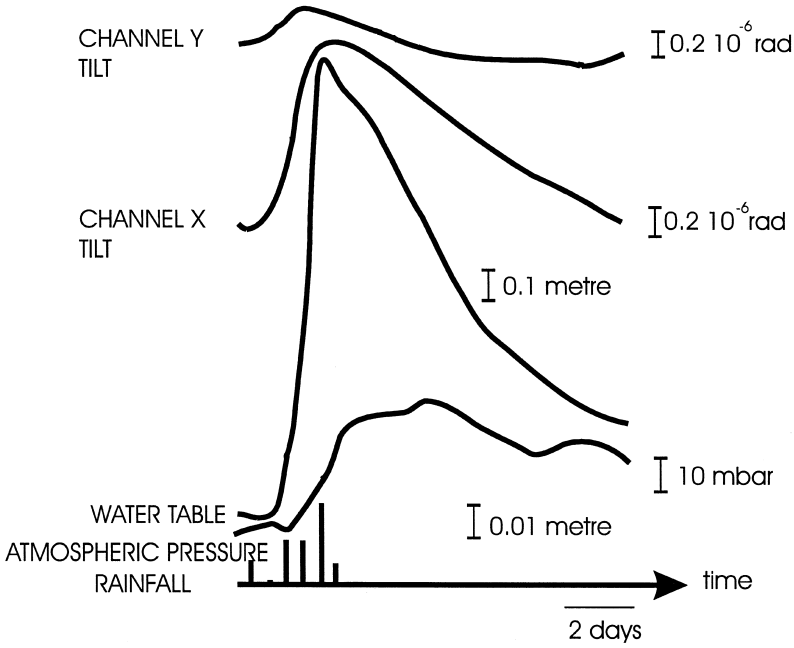

Fig. 4. Aperiodic tilt observed in an aseismic area (English Lake District). Time scale: 10th December 1977 to 21st December 1977 (from Edge et al., 1981).

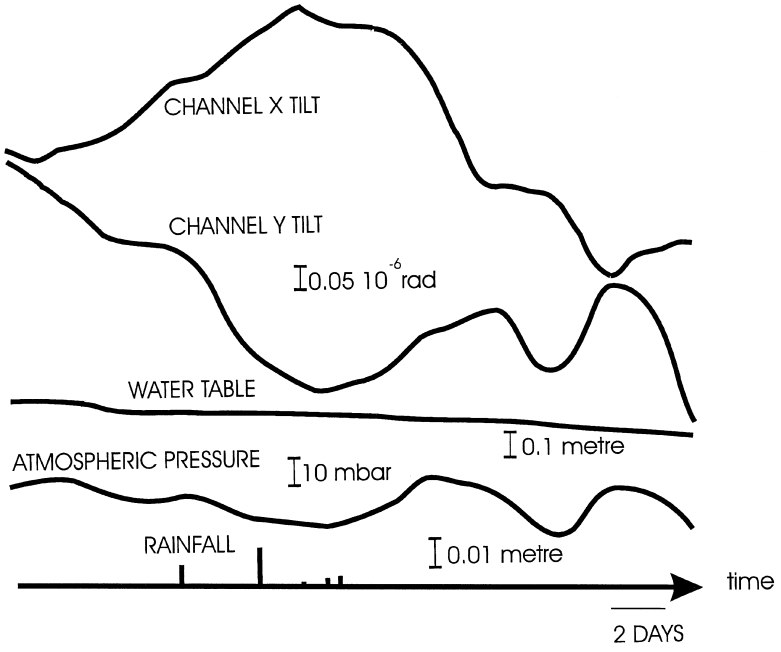

Fig. 5. Barometric induced tilt signal in the English Lake District. Time scale: 27th May 1978 to 21st June 1978. Tilt sensitivity four time greater than in Fig. 6. There is correlation of the tilt signal with atmospheric pressure (from Edge et al., 1981).

strain (3 horizontal strainmeters) and tilt data (2 horizontal pendulums) recorded since 1977 in a 60-m-deep cavity in Friuli, NE Italy (Zadro, 1992). Air pressure was found to have negligible influence on tilt in the 1/2–1/15 cpd frequency band for a data series selected over a long period without rain. The air pressure induced effect on areal strain is greater although it gives a regression coefficient of only 2 nstrain/mbar, which amounts to a maximum value of about 20 nstrain, whereas the hydrologically induced areal strain results to about 4–5 nstrain/mm (daily sampling) reaching values of up to hundreds of nstrains.

5.1. Barometric effects

In the past, attention has been dedicated to barometric effects in the context of tidal analysis, treating it mostly together with the hydrologic effect (Tomaschek, 1953; Simon and Schneider, 1967; Gerstenecker, 1986; Pagiatakis and Vaníček, 1986). Systematic research on the deformations induced by air pressure are due to Zschau (1977), Edge et al. (1981), Rabbel and Zschau (1985) and Brimich (1992). Zschau (1977) discusses the comparison of observations and theory for borehole tiltmeter observations at different depths in North Germany in the tidal frequency band. The theoretical results are obtained according to the consolidation theory in porous media of Biot (1941). The results can be summarized as follows: the air pressure effect strongly depends on the physical properties of the rocks. It increases with compressibility and decreases with the permeability coefficient (see Fig. 6). It also increases with the surface slope, the physical properties being though predominant in

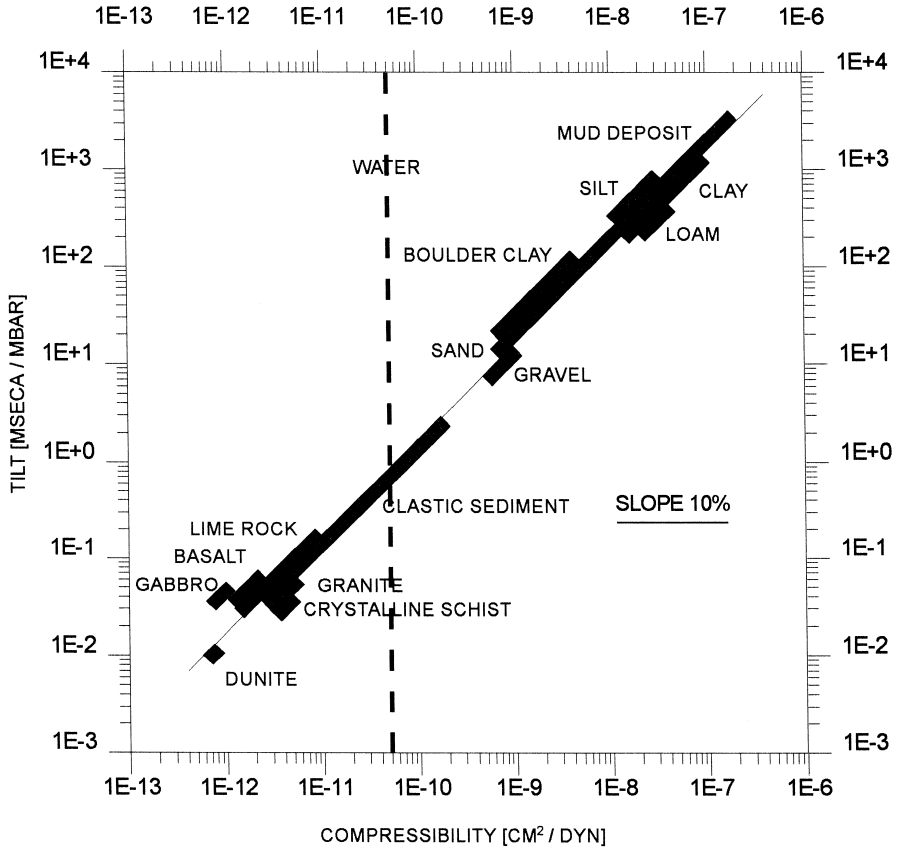

Fig. 6. Barometric tilt vs. compressibility for a 10% slope of the surface (modified from Zschau, 1977).

characterizing the effect. Considering the depth dependence, the effect is smaller above the watertable, but undergoes a sudden jump below it. The atmospheric effect is negligible below the diurnal frequency.

5.2. Hydrological effects

The quantitative description of the relation between the strain/tilt measurements and rainfall and water table variations is a difficult task and has been studied by a variety of researchers. The induced signal may also depend on whether the instrument is installed above or below the water table (Tanaka et al., 1989). The direct influence of the rainfall on the deformation measurements is difficult to quantify due to the nonlinear relationships between rainfall and ground water and to the generally poorly known behavior of the underground flow. For example, in the Friuli case the direct influence of the rainfall on tilt measurements is small as demonstrated by several analyses carried out in the past by considering a multiple input linear system (Zadro et al., 1987) with both rainfall and watertable as inputs. The ground water flow could be shown to have a remarkable influence, depending also on seasonal level variations which in this region are of the order of 10 m and over.

The induced strain signal has been attributed by several authors to changes in the aperture of subsurface hydraulically conductive fractures in response to changing fluid pressure and to compaction due to porosity changes induced by changing pore pressure (Evans and Wyatt, 1984). The hydrologic effect can influence the measurements on a broad band of frequencies, ranging from long-term and annual variations to short-period disturbances of a few hours. In both tilt and extensometric data strong rainfall is usually observed as a step-like signal followed by an exponential recovery. This characteristic may obscure possible precursory drift signals with an episodic occurrence (Wood and King, 1977). The extensometric signal is either compressive or extensive depending on the azimuth, but generally keeps a definite direction (Wolfe et al., 1981; Yamauchi, 1987). Analogously, the tilt signal has a fixed azimuth for each station. Tanaka et al. (1989) report for their tilt–strain station compression for two strainmeters and extension or compression for the third strainmeter, in accordance to a rain threshold. They also find remarkable influence of the relative depths of the instrumental installation and the subsurface levels of water runoff. Both tilt and strain signals precede the water discharge at the same depth, as could be shown from the measurement of the water discharge at several depths. The authors attribute this to the predominant effect of the faster run off of water along the surface layers above the strainmeter station, compared to the slower water discharge at depth. Also Peters and Beaumont (1981) in Québec found a strong dependence of the tilt signal on the orientation of the structures at depth, permeated by water. Long-term influences on tilt/strain have been observed by Kasahara et al. (1983), who ascribe them to fluctuations in the annual precipitation.

The modelling of the hydrologically induced signals has been tempted by different authors, with the aim of predicting the signals from observed rainfall and/or water table variations. A good approach to relating rainfall to deformation is to calculate a rainfall function (Latynina et al., 1993), given by the integral of rainfall minus a linearly increasing function:

$$r(t) = \int_0^t p(t')\,\mathrm{d}t' - \frac{\mathrm{d}\bar{p}}{\mathrm{d}t}t \tag{11}$$

The quantity $\mathrm{d}\bar{p}/\mathrm{d}t$ is equal to the average amount of rain-increment in one time unit.

The rainfall function is a much better estimate in predicting the onsets of rain-induced deformation signals than the rainfall data series itself. The physical model at the basis of the rainfall function, is the simplest possible hydrologic model of a collecting basin with an outlet. Equivalently it is possible to compare the rainfall with the time derivative of the deformation signal. In both cases, a much higher correlation coefficient is

obtained, compared to the correlation of deformation signal and rainfall. Langbein et al. (1990) define a similar rainfall function as the convolution of the daily rainfall with an exponential function with a fixed time constant, from which a linear trend is removed. The adaptation of hydrological models to the quantitative modelling of the induced strain/tilt signals has been done by Wolfe et al. (1981) who use a statistical–mathematical approach and seek the linear transfer function which relates the rainfall (input) to the strainmeter (output) response. The test carried out gives promising results, although the limited number of cases examined does not allow to draw general conclusions.

Yamauchi (1987) applies the 'tank model', a nonlinear model in which several tanks are connected in series (Fig. 7). Each tank is equipped with an intake, outlet and overflow, with which the local hydrologic conditions

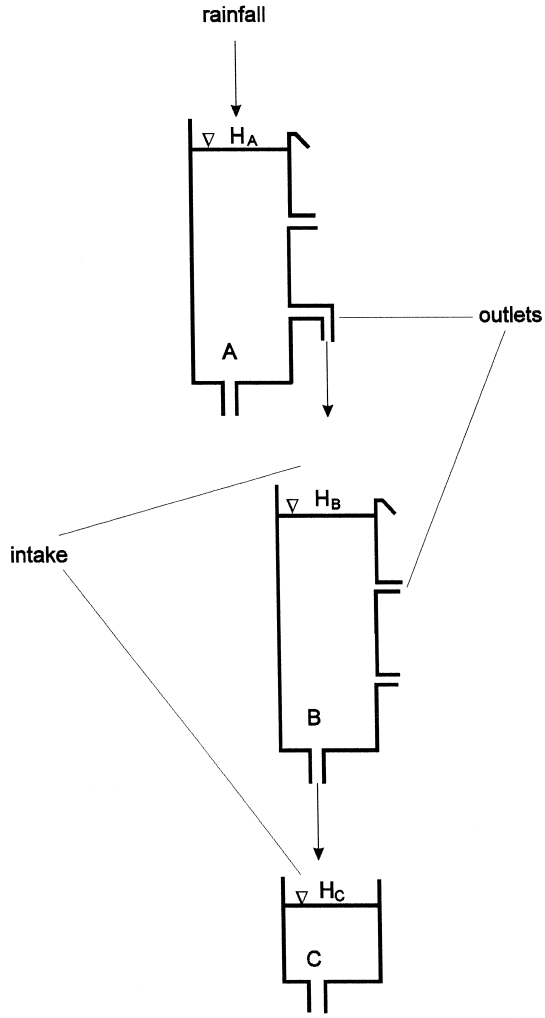

Fig. 7. Concatenated tanks (A, B, C) to simulate the hydrologic induced signal. Each tank has an intake, several outlets and an overflow. One of the outlets feeds the next tank. The observed strain change is assumed to be propostional to the water level H_c. $P(t)$ is the rainfall (modified from Yamauchi, 1987).

can be modelled. The water level of the third tank (H_c) simulates the response of strain. The parameters characterizing the tanks are determined from the data by least squares adjustment. An example is given in Fig. 8 where the rainfall, the observed (NS40), predicted (Output) and residual (Output-NS40) extensometric records are shown.

Mathematically, the problem falls into the class of linear and nonlinear predictive filtering, the theory of which can be profitably applied to this problem (see, e.g., Haykin, 1983). The method has been applied to several months of strain- and tiltmeter data, giving a good agreement between observed and predicted signals (Braitenberg and Zadro, 1994; Braitenberg, 1999).

A somewhat different deterministic approach (Kümpel, 1986; Kümpel et al., 1988) considers the physical modelling of the problem, based on controlled ground water extraction and injection experiments for well-tiltmeter configurations (Fig. 9). The model includes the mechanical elastic properties of the medium and the pore pressure at depth, according to the consolidation theory of Biot. The theory has some similarities with the work of Zschau (1977) regarding the air pressure effects. The problem may be treated by means of the finite element method, e.g., for a bidimensional plane strain or uniaxial case. Analytical solutions exist only for simple geometric configurations, like a point source in the homogeneous 3D space. The attempt is interesting but meets with some difficulties in practice, as mentioned by the authors, due to uncertainties in both the boundary conditions and the detailed local physical parameters. The theory has been applied by Weise et al. (1995, 1999) to Finnish bore-hole tilt measurements with some success.

Conclusively, although a series of approaches exist to model the hydrologic signal in deformation measurements, we are quite far from cleaning the observations from the induced signals. The problem is rather complex as it depends on soil conditions, water infiltration rate, water runoff. From the statistical point of view, the problem represents a nonlinear deconvolution problem, if rainfall or water table variations are taken as inputs.

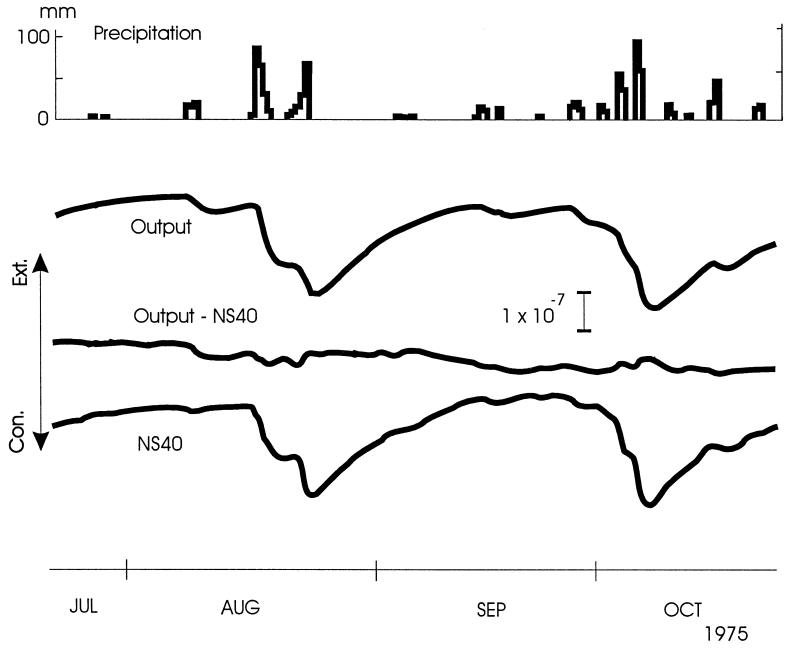

Fig. 8. Strain (NS40) signal modelled by the tank model of Yamauchi. The residual is shown in the middle curve (Output-NS40) (from Yamauchi, 1987).

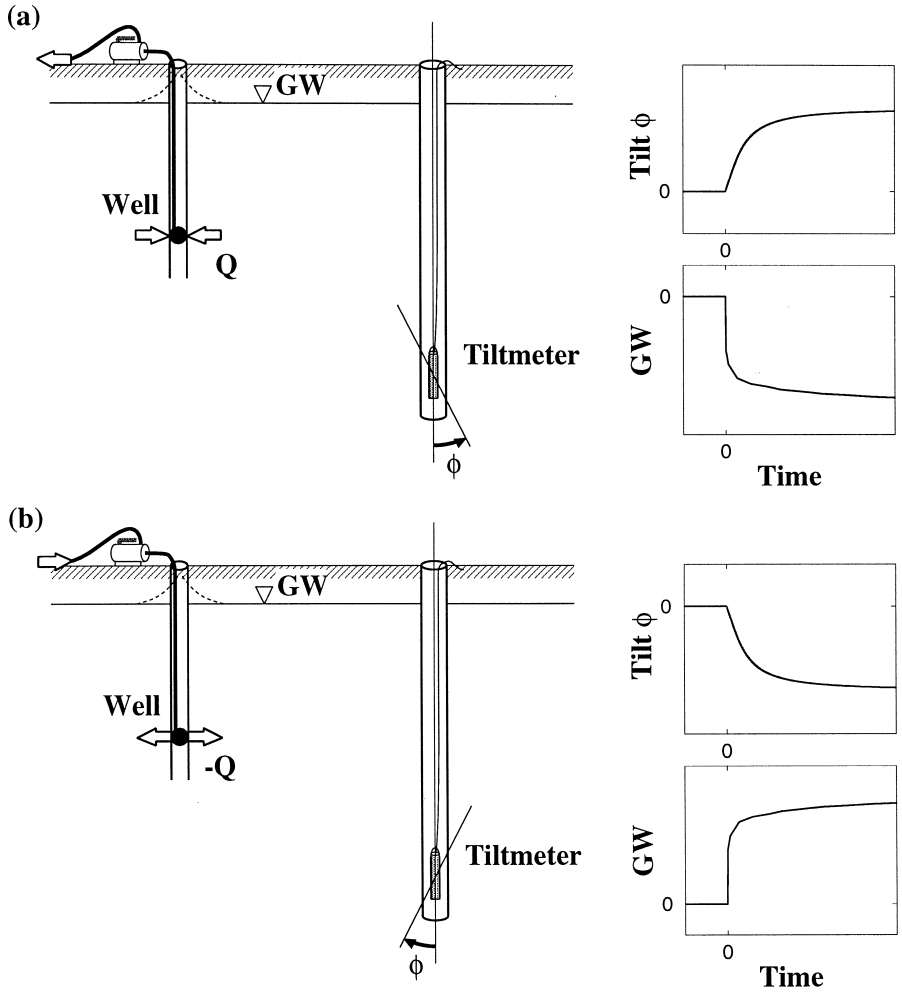

Fig. 9. Test configuration with well level (GW)/tilt signals when (a) pumping, (b) injecting groundwater at constant rate Q (sudden onset at time 0). Borehole tiltmeter is fixed to the casing (after Kümpel, 1989).

Greater results have been achieved in cleaning the observations from the barometric induced signal, and are made on a routine basis in tidal studies.

6. Short-, mid- and long-term tectonic strain variations: theoretical background and observations

Short-term variations connected to earthquakes appear in a time window of a few days centered on the occurrence time of the earthquake. Mid-term variations are defined as variations in the time window of several months (up to 12 months) centered on the earthquake. Long-term or secular variations are seen in a yearly or longer time window. Generally speaking, tectonic stress–strain variations are the cause of these deformations. In the following, we give some theoretical background of the strain signals to be expected during the entire earthquake cycle, which is divided into pre-seismic, co-seismic, and post-seismic deformation. We then show some significant observations, dividing the problem into short- to mid-term observations, that can be directly connected to the occurrence of earthquakes, and the secular observations.

6.1. Theory

The cause of the pre-seismic, co-seismic, and post-seismic signals can be of different origin, and several, conceptually differing theoretical models have been developed, which predict such strain variations.

6.1.1. Pre-seismic signals

One group of models considers the fault constitutive relations, neglecting any change in the physical properties of the crustal material. An example is the Tse and Rice (1986) model of a strike–slip fault, based on the rate and state dependent friction constitutive law. According to the authors, the model reproduces the salient features of the San Andreas fault, as earthquake periodicity, co-seismic slip, focal depth, and stress drop. Lorenzetti and Tullis (1989) chose this model to calculate the strain and strain rate distributions at different times preceding the shock. The model results are encouraging, as they suggest that sharp increases in strain rate should occur within a certain range of values of the constitutive parameters. The most useful signals to predict the earthquakes with their model turn out to be the strain changes near the fault, as the predicted strain changes are larger than the noise levels of existing borehole strainmeters. An analogous conclusion was obtained by Stuart and Tullis (1995) who model pre-seismic deformation of the Parkfield segment of the San Andreas fault.

A second group of models is based on bulk rock constitutive relations, which predict changes in the physical–mechanical properties of the material surrounding the fault. The dilatancy–diffusion model (Scholz, 1990; Scholz et al., 1973: ff 362) predicts the opening of micro cracks in the earthquake preparation zone, leading to dilatancy. Pore pressure decreases in the preparation zone, leading to water diffusion into the opened cracks from the surrounding medium. The dilatancy rate becomes high enough that pore fluid diffusion cannot maintain pore pressure, leading to dilatancy hardening, which inhibits further dilatancy. In the next stage pore pressure is re-established by fluid diffusion, followed by rupture. The growth of the number of micro cracks has influence on the elastic shear and bulk moduli, the amount being dependent on the degree of saturation of the cracks. O'Connell and Budiansky (1974) estimate quantitatively the variation of shear and bulk modulus in relation to crack density and saturation. A review on the state of knowledge concerning the elastic and dissipative properties of composite materials with small-scale inclusions or cracks is given in Hudson and Knopoff (1989). Assuming a time-constant regional stress-field, a variation in elastic parameters causes a variation in crustal strain, which in theory is observable by strain measurements. Beaumont and Berger (1974) have estimated the effect of a dilatant zone by finite element modelling on the tidal strain/tilt amplitude. They found that an elastic dilatant crustal inclusion, characterized by a 15% reduction of V_p (seismic P velocity) could lead to up to 60% changes in the tilt and strain tides. Kirsch and Zschau (1986) have studied the influence of an ellipsoidal 3D dilatant inclusion on the earth tidal field and have found that a dilating earthquake preparation zone would be accompanied by high pre-seismic amplitude variations and phase shifts.

An alternative model (Mjachkin et al., 1975; Dobrovolsky et al., 1979) developed at the Institute of Physics of the Earth, Moscow, assumes a cracked rock zone defining the fault zone. The shape and volume of the focal zone change slowly in time, due to the process of crack opening, growth, healing and redistribution. This continues until the crack concentration and the focal zone volume reach such values, that the system becomes unstable. Dobrovolsky et al. (1979) studied the deformation at the earth surface resulting from the presence of the earthquake preparation volume, which can be considered as a soft inclusion in the medium. Strains and tilts are calculated as a function of the magnitude of the forthcoming earthquake and the distance from the hypocentre. The calculations are made for a homogeneous isotropic inclusion, for which only the shear modulus decreases. Using a relative variation of shear modulus of 10%, a shear modulus $\mu = 2\ 10^5$ bar and a regional shear stress $\tau = 10^5$ bar and assuming a strain detectability limit of 10 nanostrain, the calculations predict the maximum distance R, at which a strain related to the preparing mechanisms of the focal zone should be detected:

$$R = 10^{0.43M} \tag{12}$$

M being the magnitude of the earthquake. The above relation is valid for distances greater than 2 fault length distances as in the near-field strong inhomogeneities in the produced strain field are present. According to these assumptions, the preparing mechanism for a magnitude 6 event could be detected in a radius of 380 km, for a magnitude 4 event in a radius of 50 km.

6.1.2. Co-seismic signals

Co-seismic strain signals are widely modelled by application of dislocation theory. A part of the homogeneous lithosphere is supposed to be dislocated along a finite plane. Several authors have developed the equations describing the strain field. Okada (1985) has solved the problem for an inclined fault plane in a homogeneous elastic half space. Further developments consider irregular surface topography (e.g., McTigue and Segall, 1988) and dislocations in inhomogeneous media (e.g., Du et al., 1994). Matsu'ura and Tanimoto (1980) consider the quasi static deformation due to an inclined fault in a viscoelastic halfspace.

Dislocation models allow us to estimate the distance dependence of the co-seismic signals from the earthquake source. Due to the azimuthal dependency of the strain problem, which depends sensitively on the fault-plane parameters, only an average distance-dependency may be evaluated for distances greater than a critical value. Wyatt (1988) introduces azimuthal averaging over the entire circumference at a distance R of a single strain component, or the averaging of different strain components at one site. For strike–slip faults, he finds a critical distance of about one fault size, for which to limit the strain–distance relationship. Fig. 10 gives the theoretical co-seismic strains as a function of the seismic moment or magnitude, and the hypocentral

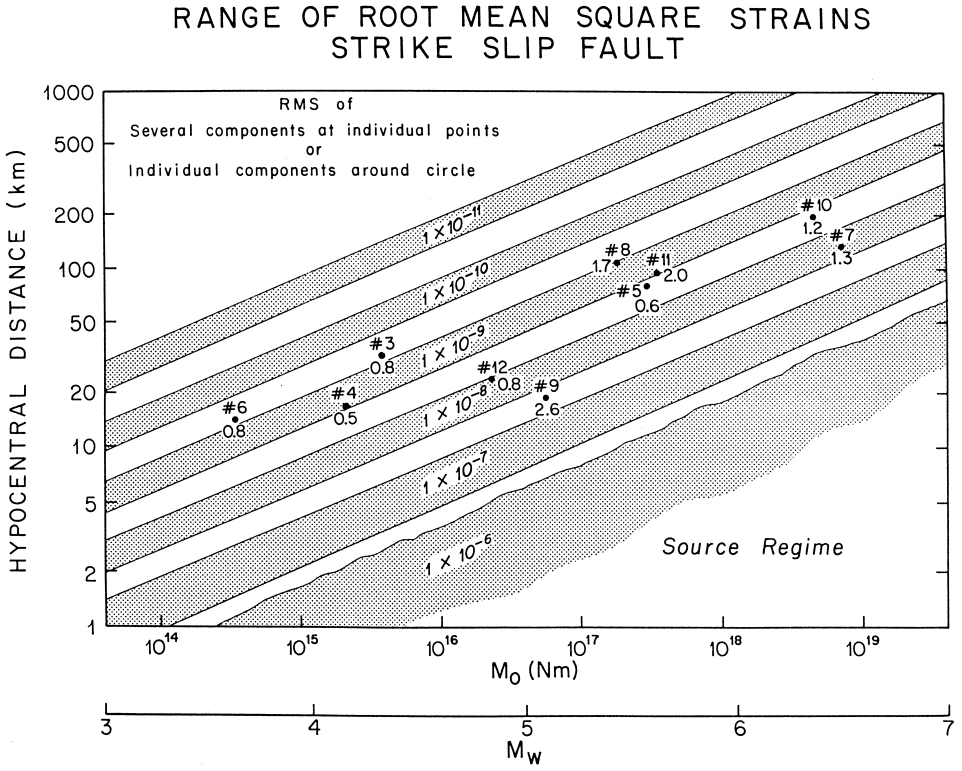

Fig. 10. Theoretical coseismic strains for a strike–slip fault (the rms of five independent strain components at on site) as a function of seismic moment or magnitude and hypocentral distance. Field observations (dots) are labeled with their event number and their ratio of the observed rms strain to the theoretical strain (from Wyatt, 1988).

distance. Field observations are labelled with an event number and their ratio of the observed strain to the theoretical strain. The event numbers refer to the Fig. 11, where all events which exceed the detection threshold (0.43 nstrain) of the Piñon Flat laser strainmeter are numbered consecutively. For distances (r) greater than the fault length, the average strain decays with the factor of $1/r^3$.

If enough strain stations are available, the fault parameters can be estimated by nonlinear least squares estimate. A systematic research on strain steps recorded in Southern California over the entire time span of 10 years (Wyatt, 1988) showed that the seismic moments obtained from seismologic records and from strain steps agree fairly well. Systematically greater moments though were estimated from the strain records. The author hypothesises that the seismologic record is not complete at low frequencies, as it does not include post-seismic fault creep. Strain steps on the other hand measure total dislocation of the fault directly. The dislocation models predict the co-seismic signals better for deep installations, than for superficial installations, the last showing often signals greater than expected.

6.1.3. Post-seismic deformation

The theoretical models of the fault preparation zone that predict strain signals preceding the earthquake, give some expectations regarding the post-seismic strain signal.

Frictional models of faulting (Tse and Rice, 1986; Lorenzetti and Tullis, 1989) predict some afterslip following the earthquake rupture on the order of 5% of the co-seismic moment in 24 h. Scholz (1990, p. 314) explains aseismic afterslip as the relaxation of a velocity-strengthening region that has been overdriven by dynamic rupture propagation into it. The afterslip is expected to decay with the law:

$$u(t) = a\log(bt + 1) + ct, \tag{13}$$

where the constants a, b, c in the equation depend on the material properties and friction.

The dilatancy–diffusion model predicts recovery of the dilatancy, at a time constant determined from the hydraulic diffusivity of the system. A recovery of shear and bulk moduli to the pre-earthquake values would be

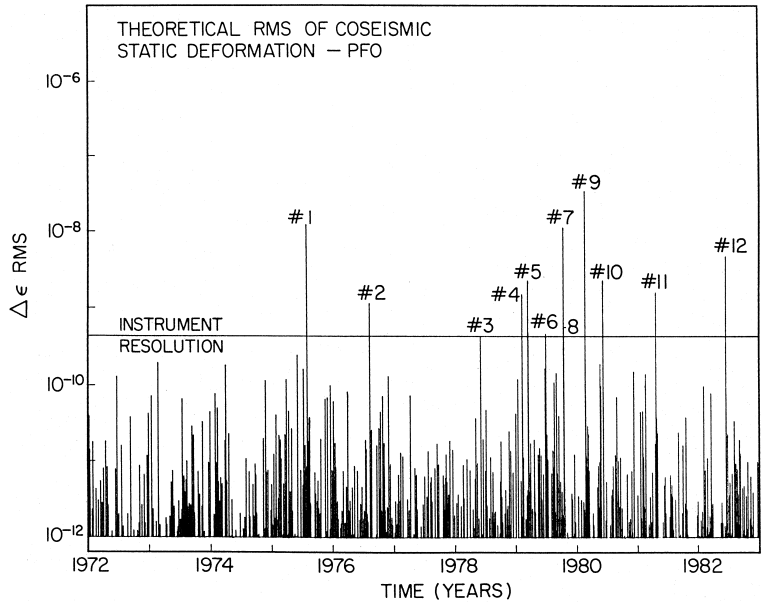

Fig. 11. Theoretical coseismic strain release at Piñon Flat Observatory, calculated on the basis of the seismic record. Earthquakes which exceed the laser strainmeter detection threshold ($\Delta > 0.43\ n\varepsilon$) are identified by event number. The same event numbers are used to identify the events in Fig. 10 (from Wyatt, 1988).

expected. Another cause can be due to the fact that the hydrologic regime may be modified in consequence to an earthquake. The re-equilibration of water pressures and watertable heights in the period following the event, can be accompanied by hydrologically induced strain signals.

6.2. Short- to mid-term observations

In the following, we have collected some strain/tilt observations which have been associated with major earthquakes.

6.2.1. California

(a) The strain field before, during and after the Landers earthquake ($M_w = 7.3$, 28 June 1992) was observed within one fault length distance (40 km distance from the greatest aftershock) by a variety of strain and tilt measuring instruments (Piñon Flat observatory), including long base laser strainmeters, GPS and geodimeter measurements (Wyatt et al., 1994). At a greater distance of 100 km a borehole dilatational strainmeter was operative at the time (Johnston et al., 1994). No pre-seismic signals were observed from either instrumentation. The observed co-seismic steps were in general agreement with the fault geometry and slip determined from either seismic data inversion or from geodetically determined ground displacements produced by the earthquake. Most interestingly a post-seismic deformation was observed on both strain and tiltmeters of Piñon Flat, characterized by initially rapid, then decaying strain changes, with the time constant of several days (see Fig. 12). The authors argue that the post-seismic strains would be due to transient creep of the upper part of the crust in response to the large stress drop imposed by the earthquake (Wyatt et al., 1994). Minor post-seismic strain is also observed by the more distant dilatometer, which could be explained by models of slip readjustment on the

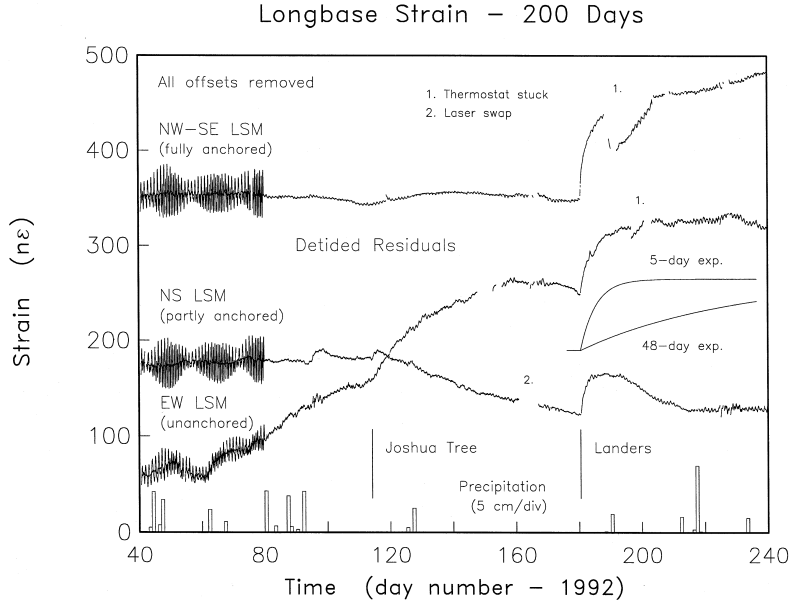

Fig. 12. Observations of the Piñon Flat long base laser strainmeters for about 5 months before and 2 months after the Landers main shock. All coseismic offsets have been removed. Due to instrument characteristics, the NW–SE strainmeter gives the most and the EW strainmeter the least stable long-term results. The large short-term fluctuations on the NW and the NS instrument were caused by a thermostat malfunction (from Wyatt et al., 1994).

Landers rupture, or by local water table pumping and readjustment following the passage of surface waves (Johnston et al., 1994).

(b) The Loma Prieta earthquake ($M_s = 7.1$, October 18, 1989) occurred not far (epicentral distance 40 km, distance to rupture < 10 km) from the installations of a borehole dilatometer and a tensor strainmeter (Johnston et al., 1990). The authors did not find any significant short-term changes during the months to minutes before the earthquake. The co-seismic steps were clearly observed (1.3 and 5 microstrain), but were not sufficient in number, to determine the source parameters of the earthquake. The comparison between the observed co-seismic deformation and that according to a dislocation model could not be made, as the calculated strain values are quite sensitive to details of complex fault geometry. These details were poorly constrained at the time by geodetic data, especially to the south of the main rupture. No significant variation in tidal amplitude was observed (Linde et al., 1992). At longer term (15 months and 5 months before the event) significant changes of strain rate were observed, accumulating up to 30% of the co-seismic step. Due to the scarcity of stations, the authors could not claim the signal to be in a definite causal link to the earthquake (Gladwin et al., 1991).

(c) The Kettleman Hills August 4, 1985 earthquake ($M_w = 6.1$) occurred 35 km NE of the intensively monitored Parkfield segment of the San Andreas fault. Three borehole dilatometers and four water wells were operative before, during and after the event. The co-seismic steps were observed by all instruments (2–9 cm water level drop in the wells, 0.1–0.7 microstrain dilatation), and have been modelled with a dislocation model of the fault. In two wells, pre-seismic level rises were observed starting 4 days before the event, of approximately equal amplitude but opposite direction to the co-seismic drop. Two of the dilatometers show pre-seismic compressional strains resembling the pre-seismic signal observed in the wells Roeloffs and Quilty, 1997). The authors claim that the pre-seismic water level and strain changes could have been produced by aseismic slip before the earthquake, where the part of the fault affected by pre-seismic slip is likely to differ from the part that slipped in the main shock.

(d) The strain observations of the Whittier Narrows earthquake ($M_L = 5.9$, October 1, 1987) by Linde and Johnston (1987) were used to invert the source parameters of the event. The co-seismic deformations recorded on several dilatometers and three laser extensometers, together with elevation changes in the epicentral area are used in the inversion. The deformation pattern is shown in Fig. 13. Units are in nstrains. The labeled dots refer to the stations used in the inversion of the fault plane solutions. The stations have epicentral distances between 47 km and 300 km. The inverted model fits all static offsets well, except for the nearest station to the earthquake, which is thought to have been affected by slip on a nearby fault, induced by the slip on the main fault. Regarding pre-seismic changes, the authors have observed that the two nearest borehole strainmeters (47 km and 66 km) showed a definite change in strain rate before the earthquake, of opposite sense to the co-seismic offsets.

(e) Johnston et al. (1987) examine the short-term strain rates preceding six Californian earthquakes, and one Japanese event recorded with near-field high resolution borehole strain and tilt-meters with the intention of verifying the existence of a nonlinear (accelerated) strain rate preceding fault failure. The shock magnitudes range from 7.0 to 3.2, with epicentral distances between just a few km to 55 km. No significant pre-seismic strain or tilt perturbations were detected. The co-seismic signals are well explained by simple elastic dislocation models, the deep borehole installations being in better agreement than near-surface installations. In several cases post-seismic deformation is observed, with a moment comparable to that of the main shock.

6.2.2. Japan

(a) A fine example of post-seismic deformation is reported by Kawasaki et al. (1995) who discuss the crustal strain observations at two stations (Esashi, 177 km epicentral distance and Miyako, 117 km epicentral distance) following the July 18, 1992 Sanriku-Oki, $M_s = 6.9$ event (Fig. 14). The post-seismic deformations are rapid in the beginning, then slowing down, with a time constant of one day. The strains are attributed to ultra-slow faulting subsequent the earthquake.

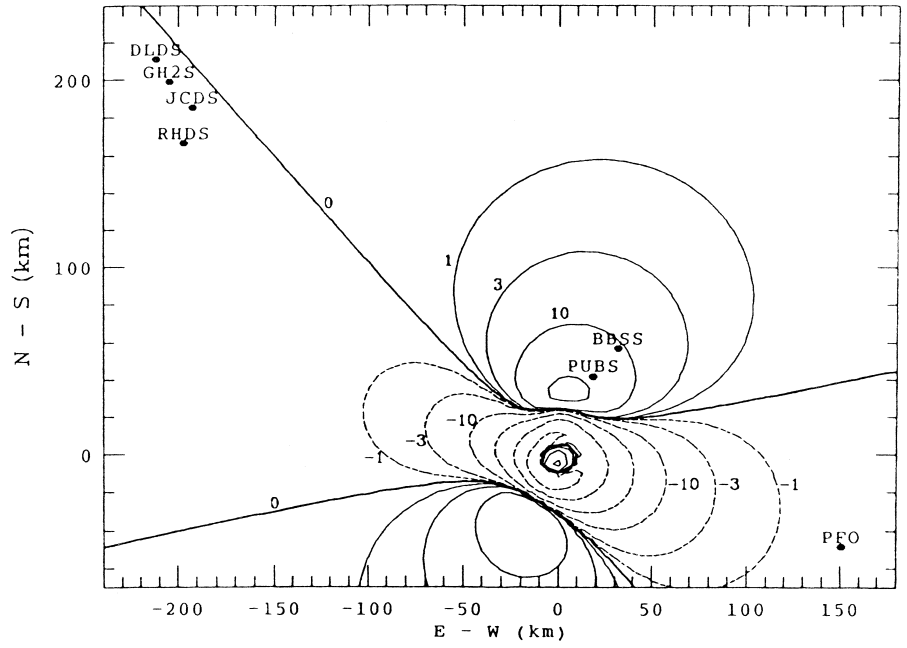

Fig. 13. Deformation for the dislocation model obtained from strain inversion of the Whittier Narrows 1987 earthquake. Isolines in nstrain (from Linde and Johnston, 1987).

(b) Ohya (1988) reports on extensometric observations which cover the occurrence time of the Hyuganada 1987, $M = 6.6$ earthquake. The strainmeter stations have distances between 63 km and 130 km from the epicenter. In this case, the great problem introduced by the hydrologically induced signals are evident. Significant pre-seismic strain is observed some time before the event, but it coincides with rainfall. Some efforts are made to correct for the hydrologically induced signals, but the effectiveness of the correction remains

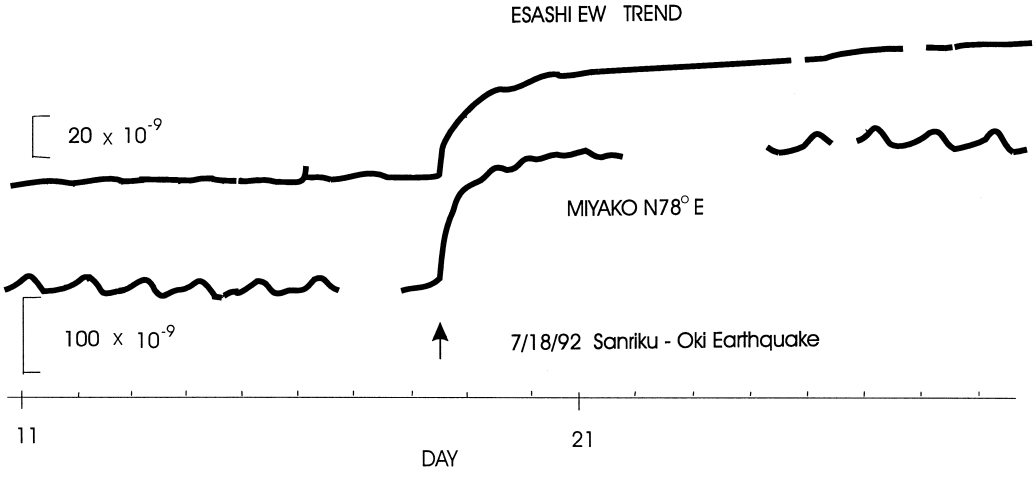

Fig. 14. Postseismic extensometer signal observed in two different stations following the Sanriku-Oki earthquake of 1992 (Kawasaki et al., 1995).

dubious. A post-seismic creep is observed on all stations, with a time constant varying from 1.4 to 8 h in different stations.

(c) Takemoto (1991) reexamines the efforts carried out in Japan to detect earthquake precursors by means of continuous crustal strain and tilt measurements. He defines a precursor to be relevant, if it has been observed simultaneously with more than two instruments or at more than two observation sites. He comes to the conclusion that with this definition no reliable precursors have been found before 1991. From his studies, he derives that a precursor may be observed if the hypocentral distance is less than about 2 source dimensions, or equivalently, less than the distance r given by $\log r = 0.51M - 1.96$, where M is the earthquake magnitude. The noise level of the strain stations is estimated to be approximately 100 nstrain, accounting for the fact that the measurements are disturbed by hydrologic factors.

In a later paper, Takemoto (1995) discusses work carried out in Japan regarding crustal deformation, including pre- and post-seismic strain and tilt changes, co-seismic strain steps and strain wave migration.

(d) The characteristics of volume strainmeters are studied bu Furuya and Fukudome (1986), using a database of 36 stations of Sacks Evertson borehole strainmeters installed throughout Japan, at depths between 50 m and 250 m. Ten stations were installed in 1976, the remainder in 1980. According to the authors, the most interesting short term strain signal was observed starting about two months previous to the 1978 Izu-Oshima Kinkai earthquake ($M = 7.0$) in one station. The signal consisted in a strain step (0.3 strain) followed 2.5 weeks later by an almost exponential signal (about 1.5 strain) for one month, ending up in the earthquake. The signal could not be assigned to a precursor, as it was only observed in one station.

(e) When writing the present review, not much was yet published in internationally accessible journals regarding the strain/tilt measurements of the $M = 7.2$ Kobe earthquake of January 17, 1995. Among 9 crustal-movement monitoring stations operating in the vicinity, none showed precursory signals, except the nearest station (King et al., 1995). This was a multicomponent borehole strainmeter operating at about 25 km distance from the epicenter at 240 m depth. It was reported to exhibit drastic strain-rate changes starting from August 1994. The variation in strain rate was accompanied by chemical changes of ground water (chloride and sulfate ion concentrations) measured in two wells 5 km distant from the strainmeter (Tsunogai and Wakita, 1995).

6.2.3. Europe

(a) Nersesov and Latynina (1992) report on the strain observations carried out in a great number of stations in the European and Central Asian regions from up to a month before and after the Spitak (Dec. 7, 1988) earthquake. The relations of the observed strain amplitudes and epicentral distances are studied.

(b) Bella et al. (1995) report on tilt measurements (Zöllner type tiltmeters) in the Italian Appennines and in Southern Caucasus (GA). They attribute anomalous tilt signals (amplitude of several rad) with time constants of up to several months to be causally related to the occurrence of small to medium ($M < 4.7$) local earthquakes. It may be objected that the ratios of epicentral distance (r) to source dimension (L) vary between 5.5 to 14, which is rather large in comparison to the observations of Takemoto, that in Japan no precursors were ever observed at distances greater than twice the source dimension. The tilt signals are attributed to aseismic creep in thrust faults close to the tilt sites. The signals are modelled assuming the crust to be consisting of rigid blocks separated by strongly cracked zones (faults). The latter exhibit viscous material properties. The stress condition is set to be constant for a certain time interval, after which it goes to zero.

(c) An estimate of the number of co-seismic signals which should have been observed in any of the stations of the Friuli (NE-Italy) tilt–strainmeter network was obtained (Dal Moro, 1997) applying the dislocation model (Okada, 1985). Among the 67 events with magnitude $M \geq 3.3$ which occurred in the time interval 1977–1993, 8 events were recorded as co-seismic steps in one or more tilt stations. Fifty percent of the observed steps had co-seismic steps more than an order of magnitude greater than expected from the dislocation model. The explanation of this discrepancy could have any one or a combination of the following reasons: the dislocation model is an oversimplification of the situation, the possible presence of aseismic creep is not resolved in the

hourly sampling rate, and could add up to the co-seismic step, locally there can be activation of superficial faults.

Two events of $M > 4$ seemed to be accompanied with anomalous strain signal before the events (Dal Moro and Zadro, 1999): in 1988 a $M = 4.1$ event was accompanied with anomalous southward drift in one station in the 2 months preceding the event. An event in 1991 was preceded by 6 days by a rapid strain signal (extension) which had been observed in two of the three strainmeters, which also coincides with the onset of strong rainfall (350 mm in one day). Although generally the induced strain signal is always compressive, in this case it was extensive.

Conclusively we may classify all the examples reported above in view of whether a pre-seismic deformation was observed and the magnitude and hypocentral distance of the earthquake. A summary of all events is listed in Table 1. In Fig. 15, the position of each event is graphed with a circle in a diagram which has hypocentral distance of the observation station on the abscissa and the earthquake magnitude as ordinate. The letters 'y' or 'n' identify whether the events were connected to presence or absence of a pre-seismic observation, respectively. The question mark '?' identifies cases in which an anomaly was observed, but the causal connection to the earthquake could not be stated beyond any doubt. The magnitude–distance relations of Takemoto and Dobrovolsky, which give the maximum distance for which a precursor signal is liable to be observed, are also included in the diagram. It can be observed that for a given magnitude, the distances at which according to Dobrovolsky a precursor could be found are much greater than those found experimentally by Takemoto. Partly, this is surely due to the fact that the noise level used for the predictions of Dobrovolsky is an order of magnitude smaller than the more realistic value found by Takemoto. In any case, it seems that the distance–magnitude relation alone is not a sufficient criterion to decide whether a pre-seismic signal should be seen or not; presumably the local conditions are so diverse, that very different situations can arise for different events.

6.3. Long-term observations

The detection and analysis of long-term strain velocity and acceleration at tectonic plate margins as well as in intra-plate earthquake-prone areas is a powerful help in the earthquake prediction strategy. It is known that rock

Table 1
Summary of the seismic events and their references discussed in this paper

Author	Locality	Date	M	d	Preseismic
Bella et al. (1995)	Central Appenines	Apr-3-91	3.3	8	y
Bella et al. (1995)	Central Appenines	Jul-13-91	3.7	36	y
Bella et al. (1995)	Central Appenines	Aug-25-92	3.9	23	y
Bella et al. (1995)	Central Appenines	Jul-16-93	3.5	28	y
Dal Moro (1997)	Friuli	Sep-16-77	5.2	8	n
Dal Moro (1997)	Friuli	Feb-1-88	4.1	2	y?
Dal Moro (1997)	Friuli	Oct-5-91	3.9	3	y?
Johnston et al. (1987)	Coalinga	May-2-83	6.7	51	n
Johnston et al. (1987)	Kettleman Hills	Aug-4-85	5.5	34	n
Johnston et al. (1987)	Morgan Hill	Apr-24-84	6.1	55	n
Johnston et al. (1987)	S. Juan Bautista	May-26-84	3.2	3.2	n
Johnston et al. (1987)	Punchbowl	Oct-31-85	3.7	7	n
Johnston et al. (1987)	Round Valley	Nov-23-84	5.8	54	n
Johnston et al. (1990)	Loma Prieta	Oct-18-89	7.1	40	n
Gladwin et al. (1991)	Loma Prieta	Oct-18-89	7.1	40	y?
Kawasaki et al. (1995)	Sanriku Oki	Jul-18-92	6.9	174	n
Kasahara et al. (1983)	Nemuro Peninsula	Jun-17-73	7.7	250	y?
Linde and Johnston (1987)	Whittier Narrows	Oct-1-87	5.9	66	y
Roeloffs and Quilty (1997)	Kettleman Hills	Aug-4-85	6.1	35	y
Ohya (1988)	Hyuganada	Mar-18-87	6.6	63	y?

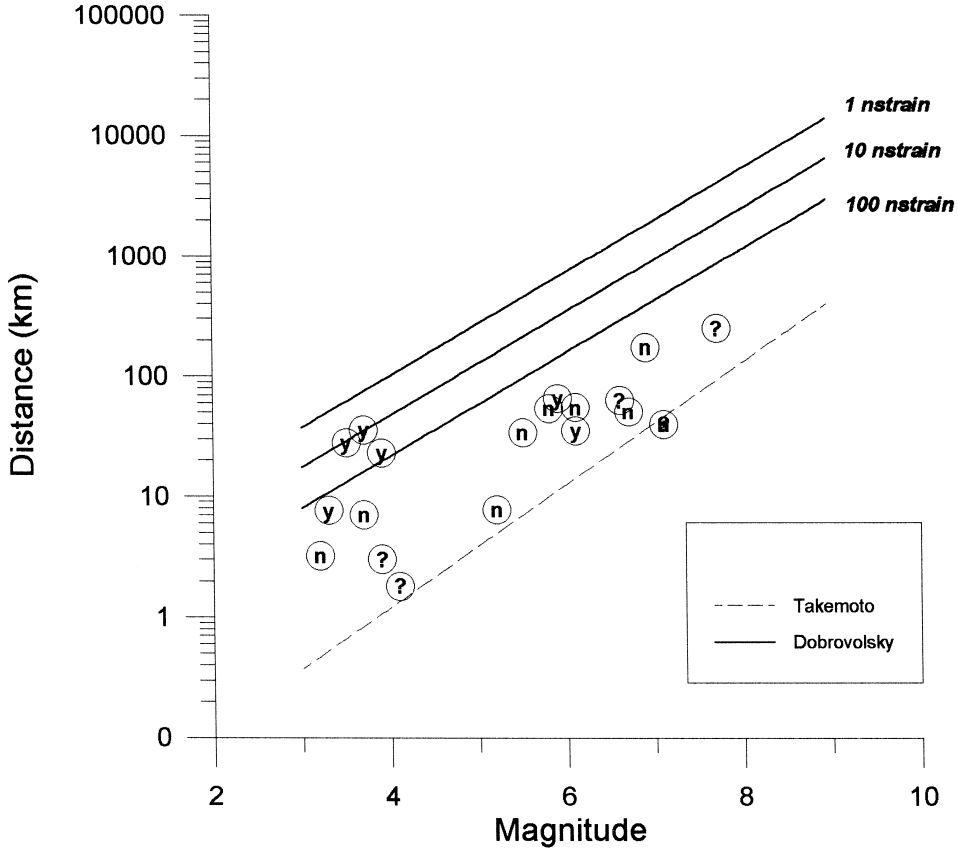

Fig. 15. Detectability limit from pre-seismic strain signals according to the theory of Dobrovolsky et al. (1979) (continuous line) and the observations of Takemoto (1991) (broken line). Takemoto assumes the noise level to be 100 nstrain. The circles show the positions of the events discussed in the present paper and summarized in Table 1: 'y' or 'n' identifies events with or without preseismic anomaly, respectiviely. '?' indicates observation of an anomaly, which though could be due to other cause than the earthquake.

fractures occur, mostly due to shearing, when the crustal strain accumulation exceeds a threshold of about 10^{-4}. The 'normal' strain accumulation in seismic active areas generally reaches values of the order of 10^{-7}/year. This is the so-called 'secular' or long-term effect. It is revealed by classical geodetic methodologies (triangulation, trilateration, levelling), by more recent geodetic techniques (GPS, VLBI, SLR) or by point-measurements (strainmeters, extensometers, tiltmeters).

The geodetic measurements give relative displacements across and along faults, more generally between pairs of surface points in a certain network, and are not continuous in time. Such data have been and are very useful in the detection and study of long-term effects, inasmuch as many geodetic repeated measurements dating back several decades are available, whereas the point continuous observations generally cover only recent years. It has to be noted that the geodetic measurements, when interpreted in terms of strain tensor and rotation rate give mean values for large surface areas and can be in some disagreement with the point-measurements. For one, the considered crustal medium is not homogeneous and isotropic, and the point measurements give the deformational response at a single point. Moreover the strain/tilt measurements are usually carried out some tens to hundreds of meters below the surface and, as discussed in paragraph 2.3, surface observations can differ from the subsurface ones, mostly in the shearing and rotational components.

Many examples of slow horizontal and vertical displacements associated with great earthquakes in critical areas such as Japan, California, Alaska, Turkmenistan, New Zealand and Australia as detected by geodetic techniques, and in some cases also by point- deformation measurements, are given by Rikitake (1976). Thereafter, many more observations have been carried out also with more sophisticated devices, especially in California and Japan.

In California, a large number of geodetic measurements have been carried out in faulted seismogenic areas. These have shown that a large part of the strain accumulation is due to simple shear (Prescott et al., 1979). Geodetic measurements show horizontal displacement rates of the order of some cm/year, e.g., in the Imperial Valley (Larsen and Reilinger, 1992) or of some mm/year, e.g., in Owens Valley, with extensional and shear strains evaluated to be about 4×10^{-8}/year and 6×10^{-8}/year across and along the Valley (Savage and Lisowski, 1995).

Other old and recent geodetic observations in California, near the White Wolf fault, in the Kern County (Bawden et al., 1997) give shear strain rates of the order of 10^{-7}/year, and show long-term pre- and post-seismic variations in connection with the occurrence of the big 1952 earthquake ($M=7.8$). We mention here the deep borehole tensor strain measurements installed at Piñon Flat Observatory (PFO) and at San Juan Bautista in 1983 (Gladwin et al., 1987) and the long-base sensors at PFO. At PFO, the deep borehole strain data are in disagreement with the regional geodetic data, as the borehole strain-gauge gave a shear strain rate of 6×10^{-7}/year, against the 5×10^{-8}/year shear strain rate of geodetic measurements. This discrepancy was ascribed to the visco-elastic response of the rock due to the presence of the borehole. At San Juan Bautista only the angle of maximum compression could be compared to the previous geodetic and hydrofractures estimates, which was in good agreement. The secular strain rate (10^{-6}/year) was not representative for geodetic strain, since the curing process of the hole after two years of measurements was not yet complete. The long-base sensors at PFO agree with the geodetic data (D. Agnew, personal communication).

In Japan, apart from a great number of geodetic measurements showing large surface displacements which are of the order of several cm/yr (see Rikitake, 1976), since 1970 more than 100 crustal deformation monitoring stations have been operative. The instrumentation includes tiltmeters, extensometers and strainmeters which are part of a national project for earthquake prediction. An overview of the Japanese work on tilt–strain measurements can be found in Takemoto (1991, 1995). Among other studies and results, it appears interesting to mention the hypothesis of Kasahara (1979) on the deformation migration landwards from oceans, which could be related to a migration of the earthquake triggering force. This hypothesis has been formulated by the author by comparing the seismicity and the long term tilt–strainmeter data in Japan, in the southern part of Kanto and in the central Tohoku district, as well as from the study of data collected in other seismic areas such as the West Cordillera Mts. (Peru), and the Anatolian fault. From his results the migration, although depending on the local plate-boundary and crustal rheological conditions, should have a velocity of 10–100 km/year. Sato (1989) has tested the above hypothesis by numerically modeling the tectonics and the rheology for the Tohoku case, finding a higher velocity (130 km/year). Such a discrepancy might be due to uncertainties in the rheological and geometrical model considered, although Kasahara et al. (1983) and Takemoto (1995) consider the hypothesis that long-term variations in precipitation and consequent ground water flow could have influenced the previous results.

Secular strain rates observed in Japan and their contribution to earthquake prediction and earthquake source studies are discussed well by Furuya and Fukudome (1986) who also point out some discrepancy between geodetic and long-term strainmeter observational data. The above cited Japanese works emphasize the importance of tilt–strainmeter measurements in the earthquake prediction strategy. It appears though, that a dense network of stations is necessary, inasmuch as according to Takemoto (1991) it would be difficult to detect earthquake precursors at distances of more than twice the earthquake source radius.

Some interesting examples of precursors and long-term deformations were detected by tilt–strainmeters in the Friuli seismic area (NE Italy), located at the eastern boundary of the Adria plate, where two great structural systems merge and interact with each other: the Alpine system with E–W-oriented overthrusts and the Dinaric

system with NW–SE-trending thrusts. Tilt measurements at that time were made with the scope of monitoring a dam. The installations were at the surface, and thus were prone to weathering effects. Nonetheless, the measurements acquired considerable attention, due to the fact that during the three years preceding the last strong earthquake (1976, $M = 6.4$) an anomalous southward tilt totaling 3 min of arc (870 microrad) was recorded. The tiltmeters were very close to the active fault (Biagi et al., 1976; Dragoni et al., 1984–1985).

Starting from 1973, a striking and unique phenomenon of 'silent or slow earthquakes' was recorded by the Marussi big horizontal pendulums of Trieste (TS), about 100 km southwards from the epicenter. Long-period oscillation (4–10 min) episodes resembling surface waves (Zadro, 1978) have been recorded by both components, each one of them lasting for several hours, with an increase of amplitude and occurrence frequency up to the disastrous 1976 seismic event. A comparable phenomena has been recorded in California at 25 to 45 km distances from the epicenter but starting only a few hours before the event (Wood and Allen, 1971; McHugh and Johnston, 1976). Probably, the exceptionality of the TS-instruments and their free period (6 min) as well as particular local tectonic features permitted to obtain such records. The phenomenon has been studied by using a visco-elastic model by Bonafede et al. (1983) who interpret it as slow dislocation events occurring on deep fault sections, where the rheological properties of fault gouge play a dominant role.

The TS data have been correlated with something more than a decade of data recorded by the tilt–strainmeter network (five two-component Marussi-tiltmeter stations, one three-component strainmeter station) installed in the Friuli seismic zone 100–120 km North of the TS station. Those components which were used in the correlation analysis are plotted in Fig. 16. For this long-period analysis, the originally hourly sampling rate was reduced to daily sampling. The selection of the components was dictated by data availability, as the correlation studies require long and undisturbed records. The records refer to two tilt components and one strain component of the Villanova (VI) station, two tilt components of the Cesclans (CE) and Trieste (TS) station and the air pressure and temperature curves. The TS–VI (distance about 100 km) and the VI–CE (distance about 20 km) cross correlation amplitude spectra are computed for several azimuths and are presented in Fig. 17a and 17b, respectively. It is seen that the strain energy is polarized along two main directions, N20W at periods over 10 years and N70E at about an 8-year period. The two directions correspond to the Alpine and Dinaric horizontal compressions acting in the zone thus supporting the hypothesis of slow travelling stress–strain waves involving deep layers, in agreement with preceding research about the propagation in space and time of earthquakes and deformations (Mogi, 1968; Kasahara, 1979).

6.3.1. Long-term variations in tidal admittance and elastic properties

An interesting approach, analysing the tidal admittance variations in the search of long and middle term earthquake precursors or post- seismic effects in seismically prone areas has been attempted by many researchers (e.g., Latynina and Rizaeva, 1976; Yamauchi, 1989; Takemoto, 1991). This kind of research is based on the dilatancy theory, therefore on the temporal variability of the rheological properties of rocks in seismic zones. Spatial variations in material properties produce large perturbations in the tilt field (called geologic effect) nearby a discontinuity as observed by many authors (e.g., Kohl and Levine, 1995; Westerhaus, 1997). As theoretically demonstrated (Beaumont and Berger, 1974), the amplitude of tidal strain may change as much as 60% for a 15% reduction of seismic P-velocity in a dilatant zone. Westerhaus (1997) in the North-Anatolian Fault zone has found significant variations in the tilt tidal responses during 1988–1994. Although the data were perturbed by seasonal and secular drifts, it was possible to associate the variations to changes of effective stress due to fluctuations of internal pore fluid pressure, as could be shown taking into account seismological data.

In the extensometer case, instead of the tidal admittance, one can analyze the l/h ratio between the Shida and Love numbers l and h. The Shida and Love numbers relate the theoretical to the observed tide (Melchior and Ducarme, 1976; Braitenberg et al., 1993). In case the observations are not affected by the oceanic tide, the ratio l/h is obtained from the phase lag only, thus bypassing possible uncertainties in calibration. Although the

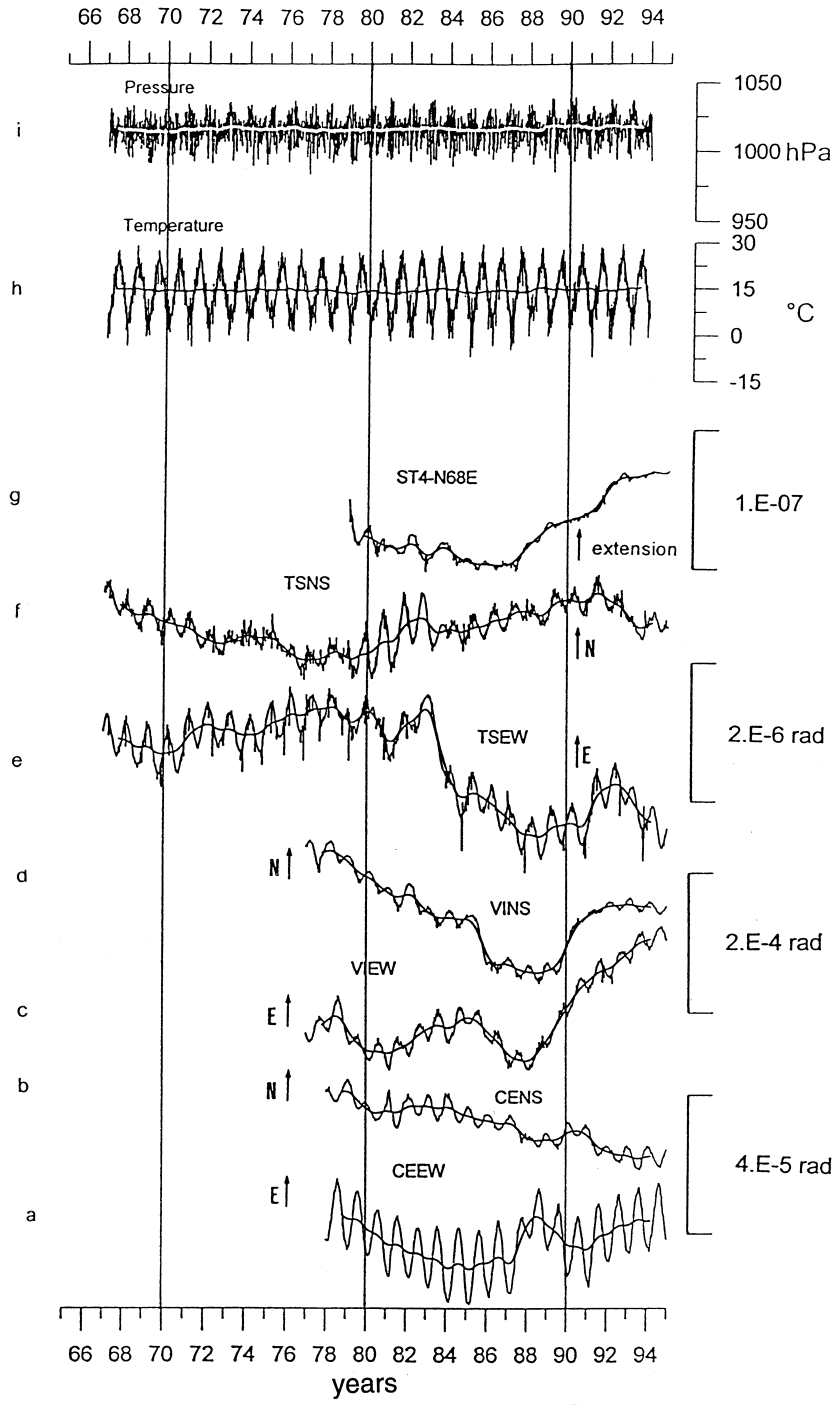

Fig. 16. Tilt and strain measurements at Grotta Gigante (TS) and the 100–120 km distant Friuli stations (VI and CE). For reference also pressure and temperature variations recorded in Trieste are shown (from Rossi and Zadro, 1996).

above-mentioned studies based on the tidal response appear as promising in the search of mechanical temporal variations in the crustal behavior, it is generally accepted by the authors that several causes mostly due to ocean loading tides and hydrological perturbations mask the effects we are looking for, so that a careful investigation of the above causes has to be carried out.

Long-term variations of the elastic parameters can be found also from the areal strain variations whenever three horizontal strain measurements are available as in the Friuli case, where the effective elastic parameters as rigidity and bulk moduli revealed a doubling of their value in the decade following the destructive earthquake of 1976 (Mao et al., 1989; Braitenberg et al., 1993), thus showing a hardening of the fracturing zone.

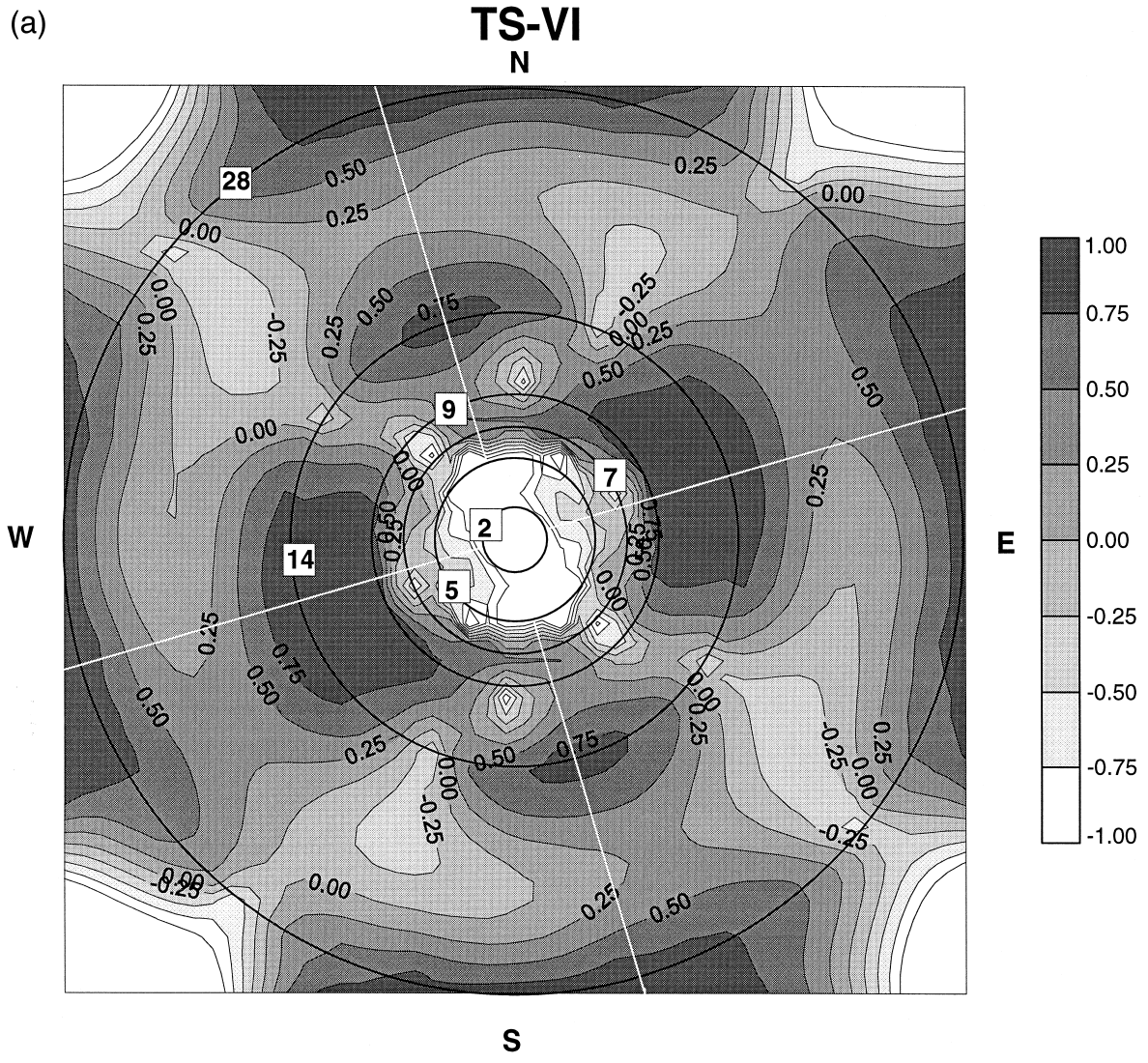

Fig. 17. Cross-correlation amplitude spectra computed for different azimuths for stations (a) TS–VI and (b) VI–CE (from Rossi and Zadro, 1996).

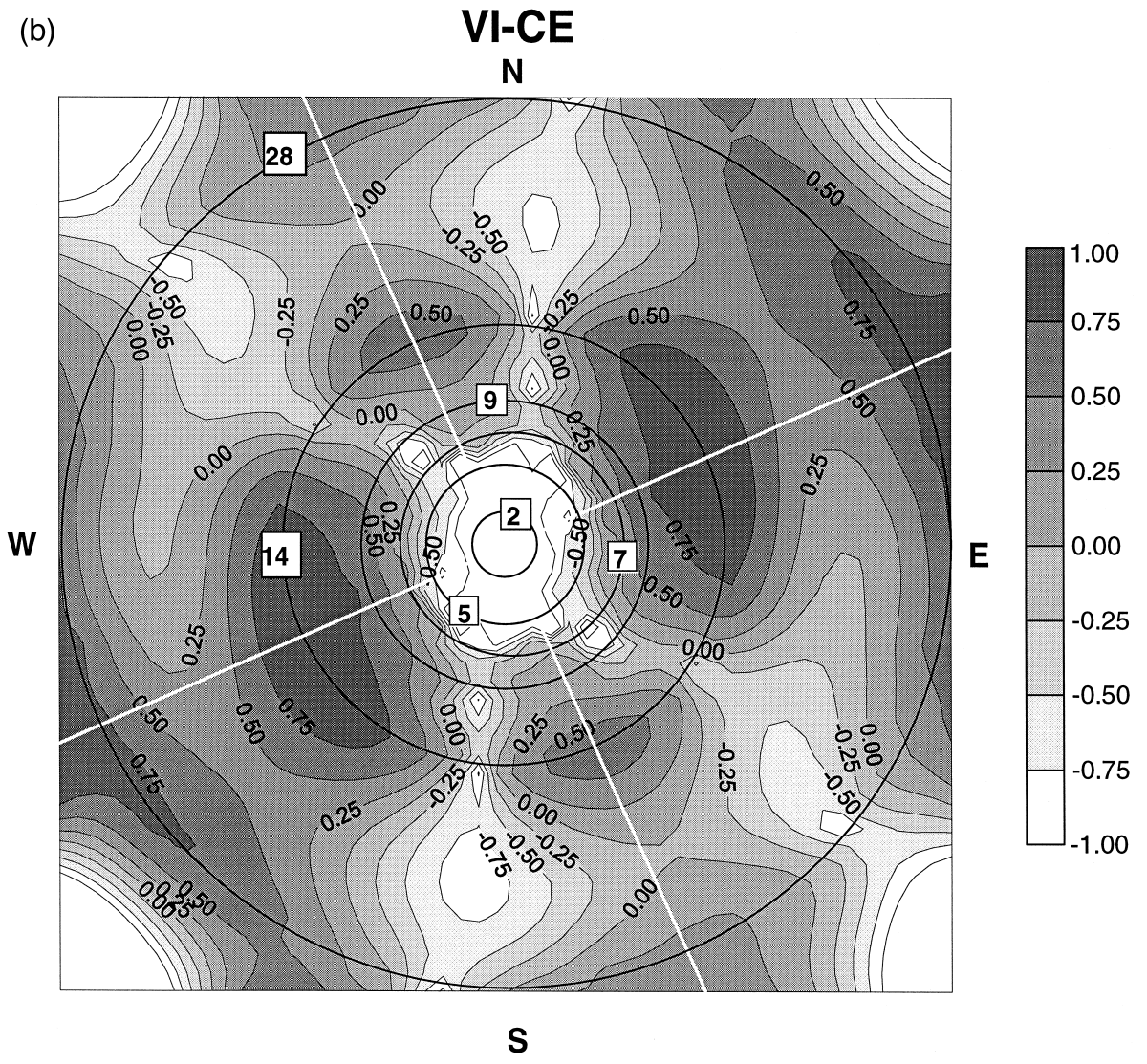

Fig. 17 (continued).

6.3.2. Seasonal variations

In the frequency range between the secular and the middle term, we have to mention also the seasonal drifts, which are recorded in almost all areas and are caused mainly by hydrological ground water and also by thermoelastic effects (e.g., Berger, 1976; Tanaka et al., 1989; Mao et al., 1990). As example we refer to Fig. 16 for the Friuli records. It also has to be added that the seasonal tilt–strain variations correspond to stress variations as well as to pore pressure variations at depth, thus justifying the hypothesis of their correlation with the local seismic activity for superficial earthquakes (Braitenberg and Zadro, 1994). This hypothesis has been put forward also by other researchers (Westerhaus, 1997), who found that the hydrologically induced stress variations can reach depths up to 10 km.

7. Concluding remarks

We have given an overview of the different aspects of observations made by strain and tilt gauges. This included theoretical considerations on the general properties of the strain field, instrument characteristics, the deformational field connected with the various stages of the earthquake cycle, and the reported observations of strain–tilt signals connected to a seismic event and long-term observations. The use of strain–tilt gauges for the prediction of earthquakes seems not to have had great success, up to the present. The earthquake-preparing mechanism should be accompanied, according to different earthquake preparation models, by a variation of the strain rate, the type of the variation being model dependent.

One problem in deformation measurements is the small magnitude of the signal, in comparison to the ambient noise level. The noise is due to non-tectonic deformations induced mainly by hydrologic, barometric and thermal agents. The least predictable, yet the most disturbing, is the hydrologically induced signal. It is nonlinearly related to rainfall and is affected by water table variations. Another problem is connected to the fact that the deformation signal decays approximately as r^{-3}, r being the hypocentral distance. The radius in which the signal is significantly greater than the noise level is generally small, compared to the sparse geographical distribution of deformation observation stations.

Future interest to monitor a seismic area, should attempt to have a possibly dense network of good quality stations. With regard to geodynamic and tectonic problems, it is desirable to have stable and continuous records in order to detect and study long term or secular deformations.

Acknowledgements

Dr. Ing. Ildikò Nagy is thanked for precious help in the management and retrieval of the references and in the drawing of some figures. Prof. C. Ebblin is thanked for valuable discussions and suggestions regarding the continuum mechanics theory. The work has been partially funded by EC research grant no. IC15 CT96-0205 and MURST ex 60%, contractor M. Zadro. The ING (Rome) is thanked for supporting the Trieste Grotta Gigante pendulums. We thank Prof. Peter Vaníček and Prof. Duncan Agnew for their meticulous reviews.

References

Agnew, D.C., 1986. Strainmeters and tiltmeters. Rev. Geophys. 24, 579–624.

Bawden, G.W., Donnellan, A., Kellogg, L.H., Dong, D., Rundle, J.B., 1997. Geodetic measurements of horizontal strain near the White Wolf fault, Kern County, CA 1926–1993. J. Geophys. Res. 102, 4957–4967.

Beaumont, C., Berger, J., 1974. Earthquake prediction: modification of the earth tide tilts and strains by dilatancy. Geophys. J. R. Astron. Soc. 39, 111–121.

Bella, F., Biagi, P.F., Caputo, M., Della Monica, G., Ermini, A., Manjgaladze, P.V., Sgrigna, V., Zilpimiani, D.O., 1995. Possibile creep-related tilt precursors obtained in the Central Apennines (Italy) and in the Southern Caucasus (GA). Pure Appl. Geophys. 144, 277–300.

Benioff, H., 1935. A linear strain seismograph. Bull. Seismol. Soc. Am. 25, 283–309.

Berger, J., Lovberg, R., 1970. Earth strain measurements with a laser interferometer. Science 170, 296–303.

Berger, J., 1976. A note on thermoelastic strains and tilts. J. Geophys. Res. 80, 274–277.

Biagi, P.F., Caloi, P., Migani, M., Spadea, M.C., 1976. Le variazioni d'inclinazione e la sismicità che hanno preceduto il forte terremoto del Friuli del 6 maggio 1976. Annali Geofis. 29, 137–146.

Bilham, R., 1981. Delays in the onset times of near-surface strain and tilt precursors to earthquakes. In: Simpson D.W., Richards, P.G. (Eds.), Earthquake Prediction, An International Review. AGU, Washington, pp. 411–421.

Biot, M.A., 1941. General theory of three-dimensional consolidation. J. Appl. Phys. 12, 155–164.

Bolt, B.A., Marussi, A., 1962. Eigenvibrations of the earth observed at Trieste. Geophys. J. R. Astron. Soc. 6, 299–311.

Bonafede, M., Boschi, E., Dragoni, M., 1983. Viscoelastic stress relaxation on deep fault sections as a possible source of very long period elastic waves. J. Geophys. Res. 88, 2251–2260.

Braitenberg, C., 1999. Estimating the hydrologic induced signal in geodetic measurements with predictive filtering methods. Geophys. Res. Lett. 26, 775–778.

Braitenberg, C., Zadro, M., Bardelli, M., Mao, W.J., 1993. Variations of tidal responses in a seismic region: the Friuli-NE Italy case. In: Hsu, H.T. (Ed.), Proc. of the Twelfth International Symposium on Earth Tides, August 4–7, 1993, Beijing, pp. 395–401.

Braitenberg, C., Zadro, M., 1994. Strains, seismicity and rain. Proc. XXIV EUC General Assembly, September 19–24, Athens, Greece, Univ. Athens, Dept. Geophysics and Geothermy, pp. 1216–1224.

Brimich, L., 1992. Air pressure and temperature influence on the extensometric measurements at the Vyhne tidal station. In: Montag, H., Reigber, C. (Eds.), Proceedings of 7th International Symposium 'Geodesy and Physics of the Earth', Potsdam, October 5–10, 1992, Springer, pp. 190–193.

Bullen, K.E., Bolt, B.A., 1985. An Introduction to the Theory of Seismology. Cambridge Univ. Press, Cambridge.

Chapman, S., Lindzen, R.S., 1970. Atmospheric Tides. D. Reidel Publishing, Dordrecht-Holland, 200 pp.

Dal Moro, G., 1997. Deformazioni crostali nell'area sismica friulana: osservazioni e modelli. Doctoral Thesis, Trieste University, 192 pp.

Dal Moro, G., Zadro, M., 1998. Subsurface deformations induced by rainfall and atmospheric pressure: tilt/strain measurements in the NE-Italy seismic area. Earth Planet. Sci. Lett. 164, 193–303.

Dal Moro, G., Zadro, M., 1999. Remarkable tilt–strain anomalies preceding two seismic events in Friuli (NE Italy): their interpretation as precursors. Earth Planet. Sci. Lett., in press.

Delorme, H., Blum, P.-A., 1991. Tiltmeter network observations at Piton de la Fournaise Volcano (Reunion Island), 1985–1990. In: van Ruymbeke, M., d'Oreye, N. (Eds.), Proceedings of the Workshop: Geodynamical Instrumentation Applied to Volcanic Areas, Walferdange, 1–3 October, 1990. Centre Europeen de Geodynamique et de Seismologie, Luxembourg, pp. 99–109.

Dobrovolsky, I.P., Zubkov, S.I., Miachkin, V.I., 1979. Estimation of the size of earthquake preparation zones. Pure Appl. Geophys. 117, 1025–1044.

Dragoni, M., Bonafede, M., Boschi, E., 1984–1985. On the interpretation of slow ground deformation precursory to the 1976 Friuli earthquake. Pure Appl. Geophys. 122, 781–792.

Du, Y., Segall, P., Gao, H., 1994. Dislocations in inhomogeneous media via a moduli perturbation approach: general formulation and two-dimensional solutions. J. Geophys. Res. 99, 13767–13779.

Dubrov, M.N., Alyoshin, V.A., 1992. Laser starinmeters: new developments and earthquake prediction applications. Tectonophysics 202, 209–213.

Eaton, J.P., 1959. A portable water-tube tiltmeter. Bull. Seismol. Soc. Am. 49, 301–306.

Ebblin, C., 1986. First estimates of the principal directions of strains compared to those of stresses in seismic Friuli, NE, Italy. Pure Appl. Geophys. 124, 897–917.

Ebblin, C., Zadro, M., 1979. On strain and tilt measurements in seismic areas. Proc. ESA-Council of Europe Seminar on Earthquake Prediction Strasbourg 5–7 March, 1979 ESA SP 149, 33–39.

Edge, R.J., Baker, T.F., Jeffries, G., 1981. Borehole tilt measurements: aperiodic crustal tilt in an aseismic area. Tectonophysics 71, 97–109.

Emter, D., Zürn, W., 1985. Observations of local elastic effects on earth tide strains. In: Harrison, J.C. (Ed.), Earth Tides. Van Nostrand-Reinhold, New York, 309–327.

Evans, K., Wyatt, F., 1984. Water table effects on the measurement of earth strain. Tectonophysics 108, 323–337.

Flach, D., 1976. Present state of the development of the Askania borehole tiltmeter. In: Szadeczky-Kardoss, G. (Ed.), Proceedings of the Seventh Int. Symp. on Earth Tides. E. Schweizerbart'sche Verlagsbuchhandlung, Stuttgart, pp. 249–258.

Furuya, I., Fukudome, A., 1986. Characteristics of borehole volume strainmeter and its application to seismology. J. Phys. Earth 34, 257–296.

Gerstenecker, C., 1986. The investigation of air pressure and temperature effects on the Hughes Borehole tiltmeter by finite element analysis. In: Vieira, R. (Ed.), Proceedings of the Tenth International Symposium on Earth Tides. Madrid, pp. 923–932.

Gladwin, M.T., Hart, R., 1985. Design parameters for borehole strain instrumentation. Pure Appl. Geophys. 123, 59–77.

Gladwin, M.T., Gwyther, R.L., Hart, R., Francis, M., Johnston, M.J.S., 1987. Borehole tensor strain measurements in California. J. Geophys. Res. 92, 7981–7988.

Gladwin, M.T., Gwyther, R.L., Higbie, J.W., Hart, R.G., 1991. A medium term precursor to the Loma Prieta earthquake?. Geophys. Res. Lett. 18, 1377–1380.

Goulty, N.R., King, C.P., Wallard, A.J., 1974. Iodine stilized laser strainmeter. Geophys. J. R. Astronom. Soc. 9, 269–282.

Groten, E., 1980. Geodesy and the Earth's Gravity Field, Vol. II: Geodynamics and Advanced Methods. Dümmler Verlag, Bonn, pp. 411–724.

Hagiwara, T., 1947. Observations of changes in the inclination of the earth's surface at Mt. Tsukuba. Bull. Earthq. Res. Inst., Univ. Tokyo 25, 27–32.

Harrison, J.C., 1976. Cavity and topographic affects in tilt and strain measurement. J. Geophys. Res. 81, 319–328.

Hart, R.H.G., Gladwin, M.T., Gwyther, R.L., Agnew, D.C., Wyatt, F.K., 1996. Tidal calibration of borehole strain meters: removing the effects of small-scale inhomogeneity. J. Geophys. Res. 101, 25553–25571.

Hast, N., 1973. Global measurements of absolute stress. Philos. Trans. R. Soc. London A 274, 409–419.

Horsfall, J.A.C., King, G.C.P., 1977. A new geophysical tiltmeter. Nature 274, 675–676.
Haykin, S., 1983. Nonlinear methods in spectral analysis. Springer, Berlin, 263 pp.
Hudson, J.A., Knopoff, L., 1989. Predicting the overall properties of composite materials with small-scale inclusions or cracks. Pure Appl. Geophys. 131, 551–576.
Jaeger, J.C., 1983. Elasticity, Fracture and flow, Science paperbacks. Chapman & Hall, London, 268 pp.
Johnston, M.J.S., Borcherdt, R.D., Linde, A.T., 1986. Short period strai ($0.1–10^5$ s): near-source strain field for an earthquake (M_L 3.2) near San Juan Bautista, CA. J. Geophys. Res. 91 (B11), 11497–11502.
Johnston, M.J.S., Linde, A.T., Gladwin, M.T., Borcherdt, R.D., 1987. Fault failure with moderate earthquakes. Tectonophysics 144, 189–206.
Johnston, M.J.S., Linde, A.T., Gladwin, M.T., 1990. Near-field high resolution strain measurements prior to the October 18, 1989, Loma prieta Ms 7.1 earthquake. Geophys. Res. Lett. 17, 1777–1780.
Johnston, M.J.S., Linde, A.T., Agnew, D.C., 1994. Continuous borehole strain in the San Andreas Fault zone before, during, and after the 28 June 1992, Mw 7.3 Landers, California. Earthquake, Bull. Seismol. Soc. Am. 84, 799–805.
Kanamori, H., 1976. Re-examination of the earth's free oscillations excited by the Kamchatka earthquake of November 4, 1952. Phys. Earth Planet. Inter. 11, 216–226.
Kasahara, K., 1979. Migration of crustal deformation. Tectonophysics 52, 329–341.
Kasahara, M., Shichi, R., Okada, Y., 1983. On the cause of long-period crustal movement. Tectonophysics 97, 327–336.
Kawasaki, I., Asai, Y., Tamura, Y., Sagiya, T., Mikami, N., Okada, Y., Sakata, M., Kasahara, M., 1995. The 1992 Sanriku-Oki, Japan, ultra-slow earthquake. J. Phys. Earth 43, 105–116.
King, G.C.P., Bilham, R., 1976. A geophysical wire strainmeter. Bull. Seismol. Soc. Am. 66, 2039–2047.
King, C.-Y., Koizumi, N., Kitagawa, Y., 1995. Hydrogeochemical anomalies and the 1995 Kobe earthquake. Science 269, 38–39.
Kirsch, R., Zschau, J., 1986. The influence of a dilatant region in the earth's crust on the earth tid tilt and strain. J. Geophys. 59, 157–163.
Kohl, M.L., Levine, J., 1995. Measurements and interpretation of tidal tilts in a small array. J. Geophys. Res. 100, 3929–3941.
Kümpel, H.J., 1986. Model calculations for rainfall induced tilt and strain anomalies. In: Vieira, R. (Ed.), Proceedings of the Tenth International Symposium on Earth Tides. Madrid, pp. 889–901.
Kümpel, H.J., 1989. Verformungen in der Umgebung von Brunnen. Habil. Thesis, Univ. of Kiel, Faculty of Mathematics and Natural Sciences, 198 pp.
Kümpel, H.J., Peters, J.A., Bower, D.R., 1988. Nontidal tilt and water table variations in a seismically active region in Quebec, Canada. Tectonophysics 152, 253–265.
Langbein, J.O., Burford, R.O., Slater, L.E., 1990. Variations in fault slip and strain accumulation at Parkfield, California: initial result using two-color geodimeter measurements, 1984-1988. J. Geophys. Res. 95 (B3), 2533–2552.
Larsen, S., Reilinger, R., 1992. Global positioning system measurements of strain accumulation across the Imperial Valley, California: 1986–1989. J. Geophys. Res. 97, 8865–8876.
Latynina, L.A., Rizaeva, S.D., 1976. On tidal-strain variations before earthquakes. Tectonophysics 31, 121–127.
Latynina, L.A., Abashizde, V.G., Alexandrov, Kapanadze, A.A., Karmaleeva, P.M., 1993. Deformation observations in epicentral areas. Fizika Zemli 3, 78–84, in Russian.
Levine, J., Hall, J.L., 1972. Design and operation of a methane absorption stabilized laser strainmeter. J. Geophys. Res. 77, 2595–2609.
Levine, J., Meertens, C., Busby, R., 1989. Tilt observations using borehole tiltmeters: 1. Analysis of tidal and secular tilt. J. Geophys. Res. 94 (B1), 574–586.
Linde, A.T., Johnston, M.J.S., 1987. Source parameters of the October 1, 1987 Whittier Narrows earthquake f crustal deformation data. J. Geophys. Res. 94 (B7), 9633–9643.
Linde, A.T., Gladwin, M.T., Johnston, M.J.S., 1992. The Loma Prieta earthquake, 1989 and earth strain tidal amplitudes: an unsuccessful search for associated changes. Geophys. Res. Lett. 19, 317–320.
Lorenzetti, E., Tullis, T.E., 1989. Geodetic predictions of a strike-slip fault model: Implications for intermediate- and short-term earthquake prediction. J. Geophys. Res. 94, 12343–12361.
Malvern, L.E., 1969. Introduction to the Mechanics of a Continuous Medium. Prentice-Hall, Englewood Cliffs, NJ, 713 pp.
Mao, W.J., Ebblin, C., Zadro, M., 1989. Evidence for variations of mechanical properties in the Friuli seismic area. Tectonophysics 170, 231–242.
Mao, W.J., Santero, P., Zadro, M., 1990. Long- and middle-term behaviour of the tilt and strain variations in the decade following the 1976 Friuli earthquake in NE Italy. Pure Appl. Geophys. 132, 653–677.
Marussi, A., 1960. The University of Trieste station for the study of the tides of the vertical in the Grotta Gigante. Proceedings of the III Int. Symposium on Earth Tides, Trieste, pp. 45–52.
Matsu'ura, M., Tanimoto, T., 1980. Quasi-static deformations due to an inclined, rectangular fault in a viscoelastic half-space. J. Phys. Earth 28, 103–118.
Meertens, C., Levine, J., Busby, R., 1989. Tilt observations using borehole tiltmeters: 2. Analysis of data from Yellowstone National Park. J. Geophys. Res. 94, 587–601.
McHugh, S., Johnston, M.J.S., 1976. Short-period nonseismic tilt perturbations and their relation to episodic slip on the San Andreas fault in Central California. J. Geophys. Res. 81, 6341–6346.

McTigue, D.F., Segall, P., 1988. Displacements and tilts from dip-slip faults and magma chambers beneath irregular surface topography. Geophys. Res. Lett. 15, 601–604.
Melchior, P., 1983. The Tides of the Planet Earth. Pergamon, Oxford, 641 pp.
Melchior, P., Ducarme, B., 1976. The ratio l/h: A simple method for the prospection of tidal deformations of cavities in the Earth's crust. Bull. Geod. 50, 137–138.
Michelson, A.A., 1914. Preliminary results of measurements of the rigidity of the earth. Astrophys. J. 39, 105–134.
Mjachkin, V.I., Brace, W.F., Sobolev, G.A., Dieterich, J.H., 1975. Two models for earthquake forerunners. Pure Appl. Geophys. 113, 169–181.
Mogi, K., 1968. Sequential occurrence of recent great earthquakes. J. Phys. Earth 16, 30–36.
Mogi, K., 1981. Earthquake Prediction program in Japan. In: Simpson, D.W., Richards, P.G. (Eds.), Earthquake prediction, An international Review. AGU, Washington, 635–666.
Mueller, R., Johnston, M.J.S., Myren, G.D., 1989. Lake level observations to detect crustal tilt: the San Andreas Lake, California, 1979–1989. Geophys. Res. Lett. 16, 661–664.
Nersesov, I.L., Latynina, L.A., 1992. Strain processes before Spitak earthquake. Tectonophysics 202, 221–225.
O'Connell, R.J., Budiansky, B., 1974. Seismic velocities in dry and saturated cracked solids. J. Geophys. Res. 79, 5412–5426.
Ohya, F., 1988. Crustal movements related to the earthquake on March 18, 1987 in Hyuganada. Bull. Disas. Prev. Res. Inst., Kyoto Univ. 38, 99–114.
Okada, Y., 1985. Surface deformation due to shear and tensile faults in a half-space. Bull. Seismol. Soc. Am. 75, 1135–1154.
Ostrovsky, 1961. Le clinomètre à enregistrement photo-électrique. B.I.M. 25, 500–536.
Pagiatakis, S.D., Vaníček, P., 1986. Atmospheric perturbations of tidal tilt and gravity measurements at the U.N.B. earth tides station. In: Vieira, R. (Ed.), Proceedings of the Tenth International Symposium on Earth Tides. Madrid, pp. 905–922.
Pearson, C.F., Beavan, J., Darby, D.J., Blick, G.H., Walcott, R.I., 1995. Strain distribution across the Australian-Pacific plate boundary in the central South Island, New Zealand, from 1992 GPS and earlier terrestrial observations. J. Geophys. Res. 100, 22071–22081.
Peters, J., Beaumont, C., 1981. Preliminary results from a new borehole tiltmeter at Charlevoix, Québec. Proceedings of the Ninth International Symposium on Earth Tides. New York City, pp. 69–77.
Prescott, W.H., Savage, J.C., Kinoshita, W.T., 1979. Strain accumulation rates in the western United States between 1970 and 1978. J. Geophys. Res. 84, 5423–5435.
Rabbel, W., Zschau, J., 1985. Static deformations and gravity changes at the earth's surface due to atmospheric loading. J. Geophys. 56, 1–99.
Rikitake, T., 1976. Earthquake Prediction. Elsevier, Amsterdam, 357 pp.
Rodgers, P.W., 1968. The response of the horizontal pendulum seismometer to Rayleigh and Love waves, tilt, and free oscillations of the earth. Bull. Seismol. Soc. Am. 58, 1384–1406.
Roeloffs, E., Quilty, E., 1997. Water level and strain changes preceeding and following the August 4, 1985 Kettleman Hills, California, earthquake. Pure Appl. Geophys. 149, 21–60.
Rojstaczer, S., 1988. Intermediate period response of water levels in wells to crustal strain: sensitivity and noise level. J. Geophys. Res. 93, 13619–13630.
Rossi, G., Zadro, M., 1996. Long-term crustal deformations in NE Italy revealed by tilt–strain gauges. Phys. Earth Planet. Int. 97, 55–70.
van Ruymbeke, M., d'Oreye, N., 1991. Design and construction of instruments adapted to volcanic zones. In: van Ruymbeke, M., d'Oreye, N. (Eds.), Proceedings of the Workshop: Geodynamical Instrumentation Applied to Volcanic Areas, Walferdange, 1–3 October, 1990. Centre Europeen de Geodynamique et de Seismologie, Luxembourg, pp. 57–70.
Sacks, I.S., Evertson, D.W., 1968. A sensitive borehole strain-rate meter. Carnegie Inst. Washington Yearbook 68, 448–455.
Sato, K., 1989. Numerical experiments on strain migration. J. Geod. Soc. Jpn. 35, 27–36.
Sato, T., Harrison, J.C., 1990. Local effects on tidal strain measurements at Esashi, Japan. Geophys. J. Int. 102, 513–526.
Savage, J.C., Lisowski, M., 1995. Strain accumulation in Owens Valley, California, 1974 to 1988. Bull. Seismol. Soc. Am. 85, 151–158.
Savage, J.C., Lisowski, M., Svarc, J.L., Gross, W.K., 1995. Strain accumulation across the central Nevada seismic zone, 1973–1994. J. Geophys. Res. 100, 20257–20269.
Schmitz-Hübsch, H., 1986. Use of a 30 m vertical tiltmeter for the detection of the actual crustal movement. In: Vieira, R. (Ed.), Proc. Tenth Int. Symp. on Earth tides, Consejs Sup. de Invets. Cientif., Madrid, pp. 855–864.
Scholz, C.H., 1990. The Mechanics of Earthquake Faulting. Cambridge Univ. Press, Cambridge, 439 pp.
Scholz, C.H., Sykes, L.R., Aggarwal, Y.P., 1973. Earthquake prediction: a physical basis. Science 181, 803–809.
Simon, D., Schneider, M.M., 1967. Zum Auftreten luftdruckbedingter Storungen in Horizontalpendelaufzeichnungen auf drei verschiedenen Erdgezeitenstationen. B.I.M. 49, 2218–2225.
Stuart, W.D., Tullis, T.E., 1995. Fault model for preseismic deformation at Parkfield, California. J. Geophys. Res. 100 (B12), 24079–24099.
Takemoto, S., 1979. Laser interferometer systems for precise measurements of ground-strains. Bull. Disaster Prev. Res. Inst. Kyoto Univ. 29, 65–81.
Takemoto, S., 1986. Application of laser holographic tecniques to investigate crustal deformations. Nature 322, 49–51.
Takemoto, S., 1990. Laser holographic measurements of tidal deformation of a tunnel. Geophys. J. Int. 100, 99–106.

Takemoto, S., 1991. Some problems on detection of earthquake precursors by means of continuous monitoring of crustal strains and tilts. J. Geophys. Res. 96, 10377–10390.
Takemoto, S., 1995. Recent results obtained from continuous monitoring of crustal deformation. J. Phys. Earth 43, 407–420.
Tanaka, T., Shimojima, E., Mitamura, K., Hoso, Y., Ishihara, Y., 1989. Precipitation, groundwater and ground deformation. In: Vyskocil, P., Reigber, C., Cross, P.A. (Eds.), Global and regional geodynamics, Edinburgh, Scotland, August 3–5, 1989, Springer, Berlin, pp. 132–139.
Tomaschek, R., 1953. Non-elastic tilt of the earth's crust due to meteorological pressure distributions. Geof. Pura e Applicata 25, 17–25.
Tse, S.T., Rice, J.R., 1986. Crustal earthquake instability in relation to the depth variation of frictional slip properties. J. Geophys. Res. 91, 9452–9472.
Tsunogai, U., Wakita, H., 1995. Precursory chemical changes in ground water: Kobe earthquake, Japan. Science 269, 61–63.
Varga, P., 1984. Long-term variations recorded by extensometers. J. Geophys. 55, 68–70.
Varga, P., Varga, T., 1995. Horizontal deformations recorded with the extensometers. B.I.M. 122, 9272–9276.
Verbaandert, J., 1962. L'étalonnage des pendules horizontaux. Boll. Geofis. Teor. Appl. 4, 419–446.
Verbaandert, J., Melchior, P., 1961. Les stations geophysiques souterraines et les pendules horizontaux de l'Observatoire Royal de Belgique. Monogr. Obs. R. Belg. 7, 1–147.
Vieira, R., van Ruymbeke, M., Fernandez, J., Arnoso, J., Toro, C., 1991. The Lanzarore Underground laboratory. In: van Ruymbeke, M., d'Oreye, N. (Eds.), Proceedings of the workshop: Geodynamical instrumentation applied to volcanic areas, Walferdange, 1–3 October, 1990. Centre Europeen de Geodynamique et de Seismologie, Luxembourg, pp. 71–86.
Weise, A., Jentzsch, G., Kääriäinen, J., Kiviniemi, A., Ruotsalainen, H., 1995. Tilt measurements in geodynamics-results from the 3-component-station Metsähovi and the clinometric station Lohja-Finland. In: Hsu, H.T. (Ed.), Proceedings of the Twelth Int. Symp. on Earth Tides, Beijing, August 4–7, 1993, pp. 105–114.
Weise, A., Jentzsch, G., Kiviniemi, A., Kääriäinen, J., 1999. Comparison of long-period tilt measurements: results from the two clinometric stations Metsähovi and Lohja, Finland. J. Geodynamics 27, 237–257.
Westerhaus, M., 1997. Tidal tilt modification along an active fault. In: Wilhelm, H., Zürn, W., Wenzel, H.-G. (Eds.), Tidal Phenomena, Lecture Notes in Earth Sciences 66. Springer, Heidelberg, pp. 311–339.
Wolfe, J.E., Berg, E., Sutton, G.H., 1981. The change in strain comes mainly from the rain: Kipapa, Oahu. Bull. Seismol. Soc. Am. 71, 1625–1635.
Wood, M.D., Allen, R.V., 1971. Anomalous microtilt preceding a local earthquake. Bull. Seismol. Soc. Am. 61, 1801–1809.
Wood, M.D., King, N.E., 1977. Relation between earthquakes, weather, and soil tilt. Science 197, 154–156.
Wyatt, F.K., 1988. Measurements of coseismic deformation in Southern California: 1972–1982. J. Geophys. Res. 93, 7923–7942.
Wyatt, F.K., Agnew, D.C., Gladwin, M., 1994. Continuous measurements of crustal deformation for the 1992 Landers earthquake sequence. Bull. Seismol. Soc. Am. 84, 768–779.
Wyatt, F.K., Morrissey, S.-T., Agnew, D.C., 1988. Shallow borehole tilt: a reprise. J. Geophys. Res. 93, 9127–9201.
Yamauchi, T., 1987. Anomalous strain response to rainfall in relation to earthquake occurrence in the Tokai area, Japan. J. Phys. Earth 35, 19–36.
Yamauchi, T., 1989. Earthquake occurrence and temporal variations in Earth tidal amplitudes. J. Geod. Soc. Jpn. 35, 149–157.
Zadro, M., 1978. Use of tiltmeters for the detection of forerunning events in seismic areas. Boll. Geod. Sc. Aff. 2 to 3, 597–618.
Zadro, M., Plenizio, E., Ebblin, C., Chiaruttini, C., 1987. Influence of groundwater table level variations and of rainfall on tilting in the Friuli area, NE, Italy. Acta Geophysica Polonica 35, 323–338.
Zadro M., 1992. Tilt and strain variations in Friuli, NE Italy, after the 1976 Eartquake. In: Boschi, E., Dragoni, M. (Eds.), Earthquake Prediction (International School on Earthquake Prediction, Erice, Italy, July 1989), Il Cigno Galileo Galilei, Roma, pp. 295–315.
Zschau, J., 1977. Air pressure induced tilt in porous media. Proc. 8th Int. Symp. on Earth Tides, Bonn, pp. 418-433.
Zürn, W., 1994. Local observation and interpretation of geodynamic phenomena. Acta Geod. Geophys. Hung. 29, 339–362.
Zürn, W., Emter, D., Heil, E., Neuberg, J., Grüninger, W., 1986. Comparison of short and long baseline tidal tilts. In: Vieira, R. (Ed.), Proc. 10th Int. Symp. Earth Tides, Cons. Sup. Inv. Cient., Madrid, pp. 61–69.

Maria Zadro is full Professor of Physics of the Earth and also teaches Geodesy at the Trieste University. She is the Coordinator of the PhD training in Geophysics of the Lithosphere and Geodynamics at the Trieste University and is active in National and International projects regarding crustal deformations in seismic areas as well as in gravity potential fields related to geodynamic processes. She is the scientific responsible of all the tilt–strain stations of the NE Italy Region cited in the present paper. Maria Zadro is author or co-author of more than one hundred papers published in international magazines, which document her main scientific interests through time: earth tides and loading effects, free oscillations of the earth, crustal deformations in seismic areas, gravimetry, isostasy and deep lithospheric structures, statistical spectral methods in treating time series as well as in gravimetric inversion problems.

With the Vordiplom in Physics of the University of Tübingen, CB accomplished the Laurea in Physics (summa cum laude) and the PhD in Geophysics at the University of Trieste. She presently holds a tenure assistant professor position at the Department of Earth Sciences of the University of Trieste. She has worked on several issues concerning the interpretation of the measurements of the strain- and tiltmeters of the Friuli (NE-Italy) strain-tiltmeter network. In particular she was interested in the observation of earth tides parameters and their variation in time, the hydrolic induced deformations and their relation to the local seismicity. A further topic of interest has been the study of the structure of crust and lithosphere applying different investigative methods which rely on the interpretation or inversion of the electromagnetic and the gravity field. Areas of study included in the Alps, the Kohistan and the Tibet-Quinghai plateau.